INTEGRATED COOPERATIVE LOCALIZATION IN VANETS FOR GPS DENIED ENVIRONMENTS

by

MARIAM ELAZAB

A thesis submitted to the

Departement of Electrical and Computer Engineering

in conformity with the requirements for

the degree of Master of Applied Science

Queen's University

Kingston, Ontario, Canada

October 2015

Dedication

To my Dad Ahmed Hossam, may his soul rest in peace.

Abstract

Accurate and ubiquitous localization is the driving force for location based services in Vehicular Ad-hoc NETworks (VANETs). In urban areas, Global Positioning System (GPS) and in-vehicle navigation sensors (e.g. odometers) suffer from prolonged outages and unsustainable error accumulation, respectively. The need for precise vehicle localization remains paramount, and cooperative vehicle localization based on ranging techniques are being exploited to this end. This research presents a novel Cooperative Localization (CL) scheme called CL KF-RISS that utilizes Round Trip Time (RTT) for inter-vehicle distance calculation, integrated with Reduced Inertial Sensor System (RISS) measurements to update the position of not only the vehicle to be localized, but its neighbors as well. We adopted the Extended Kalman Filter (EKF), to limit the effect of errors in both the sensors and the neighbors' positions, in computing the new location. In comparison to the existing cooperative localization techniques, our proposed cooperative scheme does not depend on GPS updates for the neighbors' positions thus making it far more suitable in urban canyons and tunnels. In addition, our scheme considers updating the neighbors' positions using their current inertial sensor measurements resulting in improved position estimation. The scheme is implemented and tested using the standard compliant network simulator 3 (ns-3), vehicle traces were generated using Simulation of Urban MObility (SUMO) and error models were introduced to the sensors, the initial and the updated positions. Different scenarios using different velocities and neighbors' densities were implemented. GPS updates with different percentages and error variances were introduced to test the robustness of the proposed scheme. Results show that our scheme outperforms the non-cooperative GPS and the non-cooperative RISS typically used in challenging GPS environments. Moreover, we compare our proposed scheme to a cooperative scheme based on GPS positions and demonstrate the reliability of a reduced inertial sensor system (RISS)-based cooperative scheme for relatively long time duration.

Co-Authorship

Conference Publication

M. Elazab, H.S. Hassanein, and A. Noureldin, "Integrated Cooperative Localization for Connected Vehicles in Urban Canyons," in Proc. IEEE GLOBECOM, Dec. 2015, to appear.

Acknowledgments

First of all, I would like to thank God for the endless support I got in my life and for giving me the ability to conduct my research. Secondly, I would like to express my gratitude to my both supervisors Prof. Hossam S. Hassanein and Prof. Aboelmagd Noureldin for their continuous support and guidance during my M.Sc. study and research. Your knowledge and patience helped me at all the levels of the research and during my thesis writing. Your understanding motivated me academically and personally. Thank you for everything you have done to me, your valuable feedback encouraged me to achieve better performance. It was a pleasure working with you.

I would like also to thank my examination committee members: Dr. Abd-Elhamid M. Taha and Dr. Evelyn Morin for their helpful advices and support. Thank you Dr. Abd-Elhamid for your suggestions and your constructive feedback. I was honored to have you as one of my examiners. I was also fortunate to teach the course in Queen's University with Dr. Morin. Many thanks also go to Mrs. Basia Palmer for setting me up in Canada and for giving me all the needed help in addition to her useful comments on my writing. It was a great opportunity to meet each one in the Telecommunication Research Lab (TRL), and Navigation and Instrumentation Research Lab (NAVInst). Your presentations and discussions were very beneficial.

My sincere gratitude also goes to my former supervisors at the German University in Cairo: Dr. Tallal El-Shabrawy and Dr. Mohamed Ashour for the support and guidance they gave to me during my bachelor thesis. You encouraged me to publish my first papers when I was undergraduate student. Special thanks to Dr. Hany Hammad for your great advices and for directing and helping me to continue my post graduate studies in Queen's University. All of you really inspired me with all the knowledge you had.

Since I came here to Canada, I was surrounded by amazing friends as a second family in Kingston: Rana, Gehan, Shereen, Layan, Hisham, Sherif, Anas, Mai, Mohamed Moussa, Mohamed Hosni and Mervat. I can not thank you enough for your great support. I will not forget all

the fun and the great times we had together in our gatherings and outings. My sincere appreciations go to my best friend and cheerful sister Rana Ramadan. Thanks for being with me in all the good and hard moments. You truly made a difference in my life abroad. Many thanks to my amazing friends Gehan and Shereen for your endless support to me. I am blessed to have sisters like you. Special thanks to Hisham for helping and supporting me in SUMO and ns-3.

Special thanks to my childhood friends Rana Mahmoud, Yomna, Aya Agamawy, Veronia, Marianne and Lilianne for each moment we spent together. I was fortunate to have you always by my side.

I have the best family anyone could ask for. Many special appreciations and thanks to the best mother ever, Azza Elgohary. You gave me all the support needed and you stood by my side during my whole life. You mean the world to me and I will always thank God for being your daughter. Fatma you are the best sister ever and I love you so much. I can't forget my grandmother Mona, my grandfather Salah, all my uncles and aunts: Alaa, Samah, Ihab, Ashraf, Mostafa, Ayman, Osama and Sawsan, and the rest of my family. Having you in my life is a great blessing.

To my husband Ramy Atawia, I don't find enough words to express my gratitude and appreciation to you. You are truly a gift from God. I was fortunate to have you as my soul mate, best friend and husband. Your encouragement, support, guidance, help and love made me a better person. I couldn't done this thesis without you. Thank you so much for everything.

Mariam Elazab

Kingston, ON, Canada

Sept. 2015

Table of Contents

List of Figures

List of Tables

List of Acronyms

AoA	Angle of Arrival
ARW	Angular Random Walk
CFO	Carrier Frequency Offset
CIN	Cooperative Inertial Navigation
CL	Cooperative Localization
DGPS	Differential GPS
DoP	Dilution of Precision
DR	Dead Reckoning
DSRC	Dedicated Short Range Communication
ECEF	Earth-Centered Earth-Fixed
EKF	Extended Kalman Filter
GDoP	Geometric Dilution of Precision
GNSS	Global Navigation Satellite Systems
GPS	Global Positioning System
IMU	Inertial Measurement Unit
INS	Inertial Navigation Systems
ITS	Intelligent Transportation System

IVCAL	Inter-Vehicle Communication Assisted Localization
KF	Kalman Filter
LBS	Location-Based Services
LKF	Linearized Kalman Filter
LoS	Line of Sight
LRM	Location Request Message
LSM	Least Square Method
MAC	Medium Access Control
MANET	Mobile Ad-hoc NETwork
MEMS	Micro-Electro-Mechanical System
ns-3	network simulator 3
PF	Particle Filter
RFID	Radio-Frequency IDentification
RISS	Reduced Inertial Sensor System
RMSE	Root Mean Square Error
RSS	Received Signal Strength
RSU	Road Side Unit
RTT	Round Trip Time
SINR	Signal to Interference Noise Ratio
SUMO	Simulation of Urban MObility
TDoA	Time Difference of Arrival
ToA	Time of Arrival

V2I Vehicular to Infrastructure

V2V Vehicular to Vehicular

VANET Vehicular Ad-hoc NETwork

WAVE Wireless Access in Vehicular Environments

WLAN Wireless Local Area Network

Chapter 1

Introduction

1.1 Overview and Motivation

Location-Based Services (LBS) and applications in vehicular environments are experiencing rapid development in areas such as automatic parking, safety monitoring, traffic and resource management [1]. Moreover, they have been extended to cooperative forms such as collision warning, cooperative driving and adaptive cruise control [2] and [3]. Since a high degree of positioning accuracy, in sub-meters, is a mandate of these applications, utilizing the Dedicated Short Range Communication (DSRC) is very promising. DSRC is a spectrum of 75 MHz allocated by the U.S. Federal Communications Commission in the 5.9 GHz band. As such, vehicles are allowed to communicate with each other through DSRC [4] which will enable vehicle-to-vehicle and vehicle-to-infrastructure communication in Vehicular Ad-hoc NETworks (VANETs). In particular, VANETs are considered to be an extension of Mobile Ad-hoc NETworks (MANETs) in which a group of vehicles can exchange information for different monitoring and controlling applications that can support Intelligent Transportation System (ITS). This communication is furthermore governed by the physical and Medium Access Control (MAC) protocols defined in the Wireless Access in Vehicular Environments (WAVE) in IEEE 802.11p, resulting in efficient spectrum utilization.

1.2 Challenges

Such developments in LBS and applications necessitate pervasive precise localization of vehicles. Global Navigation Satellite Systems (GNSS) such as Global Positioning System (GPS) provide location information with accuracy of 10 m. However, this level is not guaranteed in urban canyons [5] where the satellite signals typically experience excessive multipath due to high

rise buildings. Moreover, this signal requires open sky access, which is unavailable in tunnels. As a solution, a plethora of advanced positioning techniques was introduced in the literature in order to handle these outages. The most widely presented is integrating GNSS with other navigation systems such as Radio-Frequency IDentification (RFID) [6], Wireless Local Area Network (WLAN) [7] or Inertial Navigation Systems (INS), among others. INS uses Dead Reckoning (DR) to update the current position of a vehicle based on the last known position, and the current speed and the heading measurements of on-board sensors [8]. However, in GPS-free environments such as tunnels and urban canyons, the above conventional integration techniques are sub-optimal because of the extra cost required for deploying reliable infrastructures such as RFID and WLANs or due to the INS error accumulation in case of protracted GPS outages. Accordingly, cooperative localization is thoroughly addressed and anticipated to achieve the required accuracy in VANETs [5].

Vehicular cooperative localization exploits the DSRC capability and allows vehicles to update their positions using both: positions of their surrounding neighboring vehicles and, the measured inter-vehicle distance through ranging techniques. In particular, some neighboring vehicles can obtain position updates only during partial access to GPS or in the existence of nearby landmarks with known positions. These vehicles can broadcast their current accurate positions and act as mobile anchors to the other surrounding vehicles with unknown or low accuracy locations (denoted as vehicles to be localized). Afterwards, a ranging technique can be used to estimate the distance between the vehicles to be localized and their surrounding neighbors (potential anchors). The ranging techniques are typically divided into two categories [5], radio ranging and range rating techniques. Radio ranging techniques are either power-based such as Received Signal Strength (RSS) or time-based such as Time of Arrival (ToA), Time Difference of Arrival (TDoA) and Round Trip Time (RTT). On the other hand, the range rating technique is based on the Doppler shift of the received signal due to the movement of the transmitter or the receiver.

RSS is considered to be the simplest technique among all the others as it provides distance estimation based on the path loss model in Eq. 1.1. For accurate estimation of the distance between the two vehicles, the path loss exponent has to be perfectly calculated. In particular, this exponent represents the attenuation of the signal's power with the distance. However, the value of the exponent depends on the density of buildings and obstacles in the area accommodating the

transmitter and receiver. Thus, there is no guarantee to perfectly estimate such density or its effect on the received power and thus the value of the exponent can not be easily determined. As such, this simple RSS is considered the least accurate ranging technique.

$$P_r(d) = P_0 - 10n \times log(^{d}/_{d_0}) \tag{1.1}$$

Where:

- d is the distance between the transmitter and the receiver.
- $P_r(d)$ is the power of the signal received at distance d.
- P_0 is the power calculated at a reference distance d_0.
- n is the path loss exponent.

Time-based ranging techniques, provide distance calculation by measuring the duration taken by the signal in the wireless channel while considering the fact that the wireless signal travels at the speed of light. The first and simplest time-based technique is the ToA which measures the time taken by the signal to propagate from the transmitter to the receiver. The TDoA measures the difference between the time reception of two signals at the receiver from two synchronized transmitters. ToA and TDoA can provide accuracy to within a few meters, however at the expense of their complexity as they require transmitter and receiver synchronization and they are easily affected by the multipath as in GPS. For this reason, both ToA and TDoA cannot be used in VANETs. RTT is then considered to be the best compromise as it does not require synchronization between the transmitter and the receiver and thus provides good accuracy with lower complexity. It estimates the distance by calculating the round trip time at the transmitter. The main challenge in RTT is the processing delay at the vehicles. However, this delay can be minimized by decreasing the localization overhead in the network and so, fast processing of data is guaranteed. Such processing time can be also statistically modeled and compensated in the calculations [9] resulting in high accuracy range estimation [10].

Range rating techniques based on Doppler shift calculation provide distance estimation between the transmitter and the receiver using Carrier Phase Offset (CFO) which represents the difference between the transmitted and the received frequency of the carrier signal. The main ad-

vantage of this technique is that it is not affected by obstacles as in the radio ranging techniques. However, the Doppler shift information is usually affected by the clock drifts in the CFO measurements and also requires a high value of relative velocity between the transmitter and the receiver [5].

Furthermore, the Angle of Arrival (AoA) technique can be used to detect the direction of the received signal using antenna arrays. Thus, it can be combined with radio ranging or range rating techniques to compensate the multipath and synchronization effects. This provides high accuracy, however at the expense of the cost of the added antennas and the computational complexity required for the signal processing of used antenna arrays.

To summarize, the accuracy of the first cooperative information (i.e. neighbors' positions) depends on the localization technique used to obtain the neighbor's position. In addition, the second cooperative information (i.e. inter-vehicle distance) is subject to different sources of errors according to the used ranging technique. Therefore, the main challenges for a reliable and accurate cooperative localization are: 1) choosing the localization scheme and the ranging technique suitable for the environment, 2) mitigating the associated errors in both location and range, and 3) selecting the data fusion method for integrating the above mentioned data. Our proposed cooperative localization scheme uses the RTT ranging technique and integrated with sensors-based localization technique such as INS, to update the neighbors' positions during GPS outages. The final accurate position is then estimated by adopting Extended Kalman Filter (EKF) which fuses the above data with the recent position of the vehicle to be localized (obtained from INS).

1.3 Objectives and Contributions

The aim of this work is to introduce a VANETs distributed cooperative localization scheme to be used in urban canyons and tunnels where there is a complete GPS blockage and infrastructure-based localization is unfeasible. Accordingly, only on-board vehicle sensors and inter-vehicle communication are used to update the vehicles' positions throughout their trajectory.

To overcome the above mentioned drawbacks, our scheme applies RTT which does not require synchronization since the same vehicle will be calculating the difference between the time of transmission and reception. Moreover, RTT is proven to be robust to the channel and synchronization errors for measuring inter-vehicle distances [11].

Unlike previous schemes, ours updates the neighbors' locations through their on-board sensors/INS readings prior to using these locations in localization. To ensure the robustness of our scheme, both the INS sensors and the initial position errors are considered and modeled as normally distributed random variables. Accordingly, a linearized EKF was used to integrate the measured inter-vehicle distances along with INS readings to estimate accurate positions for the vehicle to be localized in the presence of the above erroneous data.

We evaluate our introduced scheme using extensive simulations using standard compliant network and legitimate traffic simulators. Simulation of Urban MObility (SUMO) is adopted to generate practical traffic scenarios that model the vehicles' movements. These traces are further imported by the network simulator 3 (ns-3) where the cooperative scheme is implemented using WAVE protocol for practical communication between moving vehicles [1].

The work presented in this thesis is organized as follows: Chapter II contains a background of the widely used conventional localization techniques as well as the existing non-cooperative and the cooperative schemes. Chapter III provides an overview of the implemented distributed cooperative scheme while Chapter IV introduces the detailed implementation of the system modules. The simulation environment and the performance evaluation is then provided in Chapter V. Lastly, Chapter VI summarizes and concludes the work in addition to providing recommendations for the future work.

[1] Part of this work is accepted to be published in [12].

Chapter 2

Literature Review on VANETs Localization

2.1 Conventional Localization Techniques and Integration using Kalman Filter

Localization, in general, refers to finding the position of the vehicle in the global coordinate system. Most vehicles nowadays are equipped with both GPS and INS that allow self-localization of the vehicle. The GPS typically requires direct Line of Sight (LoS) to GPS satellites in order to calculate the current position. Nevertheless, the accuracy of such position depends on the availability of the satellite's LoS signal in addition to other factors such as satellite geometry, multipath effect, and receiver noise. In urban canyons and downtown areas, as illustrated in Fig. 2.1, the above requirements for GPS are not satisfied as the signals are either blocked or suffer from multipath effect due to high rise buildings. For this reason, localization through standalone GPS does not guarantee ubiquitous positions. Thus INS is typically used in these scenarios to obtain position based on the motion sensors' measurements. Although INS is not sensitive to the environment as in GPS, the former suffers from error accumulation over time due to the dead reckoning technique used to obtain the vehicle's position [8]. Accordingly, GPS/INS integration appears as a promising solution for ubiquitous localization in urban canyons.

2.1.1 Global Positioning System (GPS)

GPS is a satellite-based navigation system launched by the US Department of Defense for the first time in 1978 [8]. This navigation system can provide both position and velocity for the objects of unknown positions using the signal received from the satellites. The GPS network consists of at least 24 satellites that are circulating in six orbits around the earth. To determine the 3D position (longitude, latitude and altitude) and velocities of any object with a GPS receiver, information

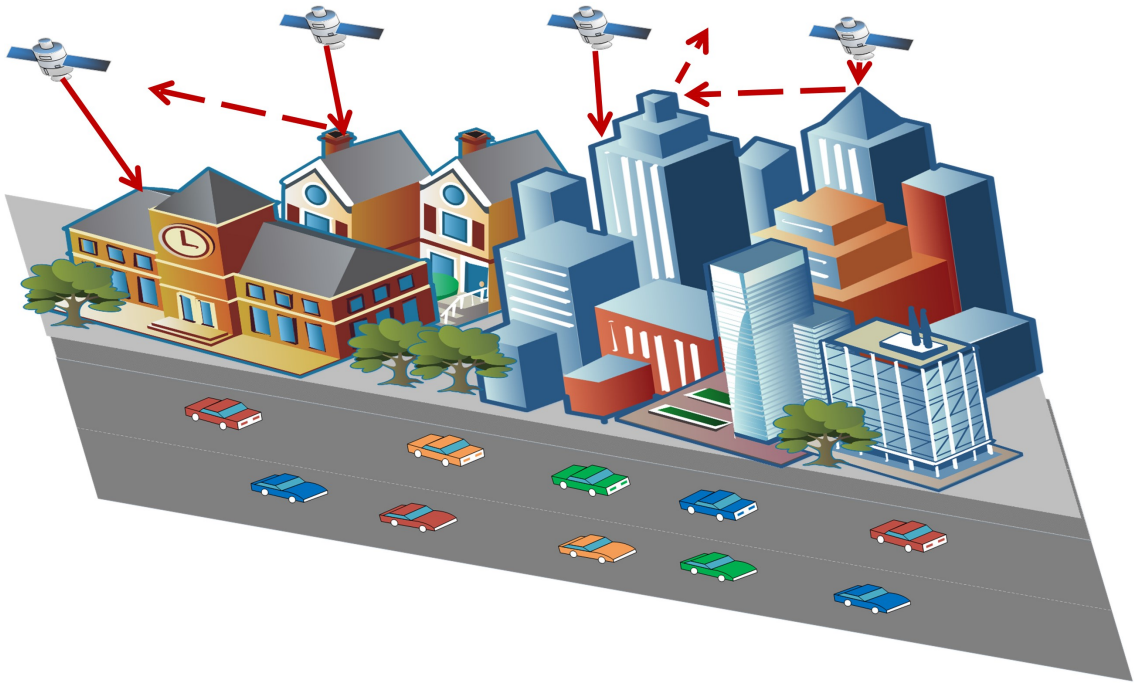

Figure 2.1: Urban area with GPS blockage and multipath

(e.g. distances) from at least four satellites is required to apply the trilateration/multilateration localization technique [13] as shown in Fig. 2.2. The three main measurements transmitted from the satellites to the GPS receiver are the pseudorange, carrier phase and doppler shifts.

The pseudorange measurements represent the distance between the satellite itself and the GPS receiver. This distance can be also calculated using the carrier phase measurements of the signals. This latter calculated distance is more accurate than the one obtained from the pseudorange measurements. It can be computed using the wavelength of the carrier and the total number of cycles of the signal between the satellite and the receiver [8]. On the other hand, the velocity of the receiver is calculated from the Doppler frequency shift in the signal resulting from the relative mobility between the transmitter (satellite) and the GPS receiver.

The ranging measurements from the satellite signals experience several errors that will affect the position calculation accuracy. Some of these errors can be compensated and mitigated such as satellite clock, receiver clock and ionospheric errors. Others cannot be perfectly calibrated as the tropospheric, satellite orbital, receiver noise errors and multipath which has a direct impact on the accuracy of the obtained position. The multipath effect causes the signal to be reflected leading to the degradation in the position accuracy since it can reach the source with different

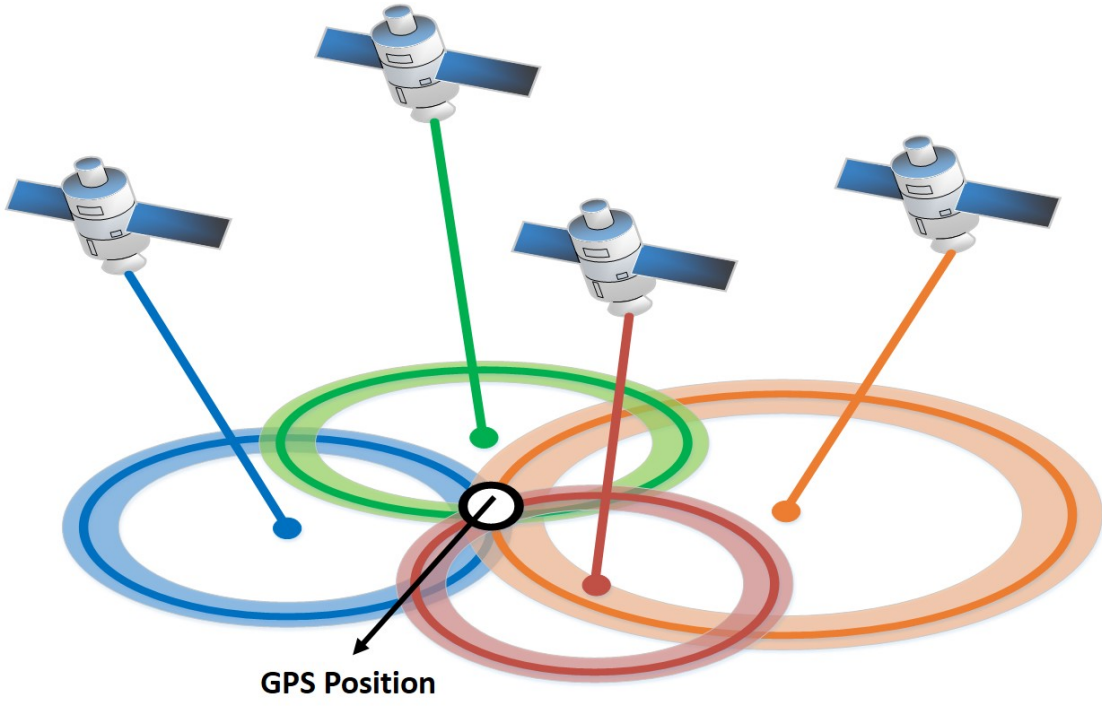

Figure 2.2: Trilateration based GPS position with no errors in satellites signals

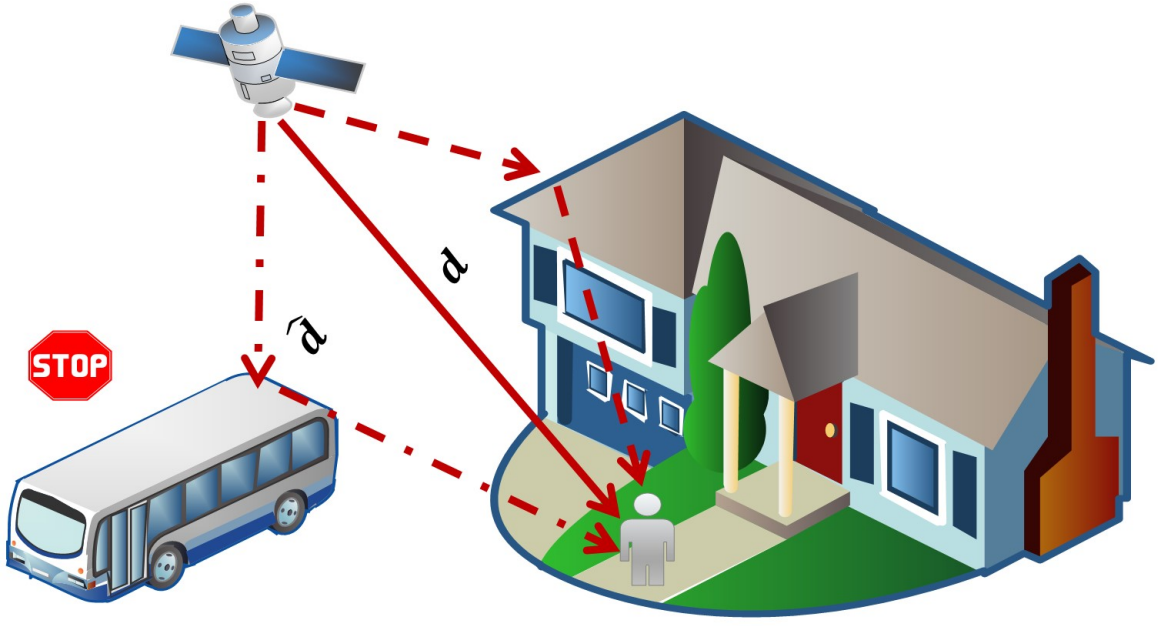

Figure 2.3: Multipath of the satellite's signal

paths beside the LoS as shown in Fig. 2.3. Accordingly the measured distance $\hat{d}$ does not reflect the actual distance d between the GPS receiver and the satellite resulting in an inaccurate position. The geometry of the satellites compared to the receiver also affects the position accuracy which

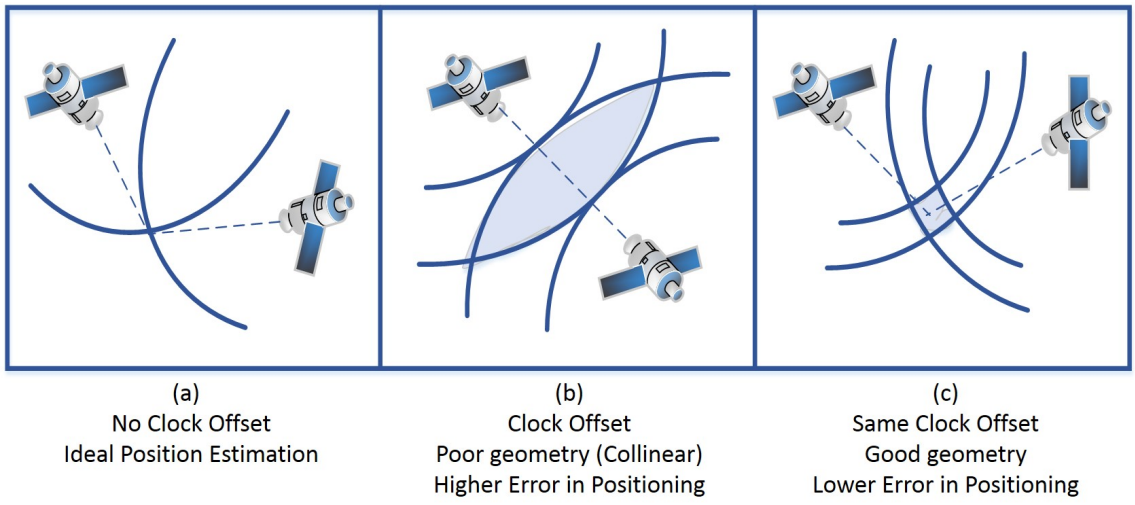

Figure 2.4: Different GDoP values

is represented by a value called Geometric Dilution of Precision (GDoP) as illustrated in two dimensions in Fig. 2.4. The intersection between the erroneous satellites' signals is a plane area in which its size represents the uncertainty in the position that increases with the GDoP value. In particular, good relative geometry between the satellites and the user receiver (e.g. satellites at right angles relative to the receiver) reflects a smaller intersection area which means a smaller Dilution of Precision (DoP) value and thus a lower error value in the position estimation as shown in Fig. 2.4 (c).

Since these measurements from the satellites suffer from the aforementioned errors, Least Square Method (LSM) or Kalman Filter (KF) which will be introduced later are typically used to provide the position that minimizes the difference between the sum of the residuals. Thus, four satellites are required by the linearized models to obtain the 3D position and the receiver clock bias which resulted from the non-synchronization between the satellite and the receiver clock.

The position accuracy measured using GPS can reach an error of 10 to 15 m [8]. However, in urban areas of dense high rise buildings, satellite signal blockage and multipath may lead to deterioration in the positioning accuracy and eventually complete absence of the positioning solution. Thus, GPS error increases in these situations resulting in non-acceptable accuracy for most of the safety applications mentioned in Section 1.1. Accordingly, another localization system is used to help the GPS in case of obstructions in urban canyons which is the INS introduced earlier and will be discussed in the next section.

2.1.2 Sensors-Based Localization and Dead Reckoning

2.1.2.1 2D/3D INS

INS is used to provide the position, velocity and attitude for a certain vehicle based on the DR concept using the measurements from three axis accelerometers and three axis gyroscopes. In particular, INS contains an Inertial Measurement Unit (IMU), pre-processing component and mechanization unit. The IMU contains three orthogonal accelerometers which are responsible for measuring the acceleration in three orthogonal directions (x , y and z) and three orthogonal gyroscopes for measuring the rotation angles. While for 2D navigation, only two accelerometers and one gyroscope are enough. The second component in INS is the pre-processing unit and it is responsible for filtering the measurements of the accelerometers and gyroscopes.

After that, INS mechanization is performed to process the on-board sensors' measurements and the last known position. By double integrating the measured acceleration, the displacement between the last known position and the current unknown position is determined. Moreover, the angular rotations monitored by the gyroscopes are processed to determine the vehicle's orientation and the heading, and thus the position of the vehicle can be calculated. This system is mainly used in urban canyons with total blockage where GPS is unavailable as in tunnels to provide an accurate position estimate, but only for a short time before it starts to deviate.

Generally, both gyroscopes and accelerometers suffer from systematic and stochastic errors that will degrade the performance of localization. Commonly, the systematic errors can be calibrated and compensated while the stochastic errors are modeled to be mitigated through the use of optimal estimation like KF [8]. The main metrics to measure the performance of an IMU are the gyroscope and the accelerometer bias drifts that represent the stability of the sensor bias expressed in deg/hr and m/s^2, respectively; and as well the gyroscope random walk which is expressed in $deg/\sqrt{hr}$ which represents the random noise of the sensor. For consumer applications, most of low-cost gyroscopes used nowadays are manufactured using Micro-Electro-Mechanical System (MEMS) technology. Even if the errors values are small, they are magnified and accumulate through double integration and thus can reach unsustainable levels over a long period of time.

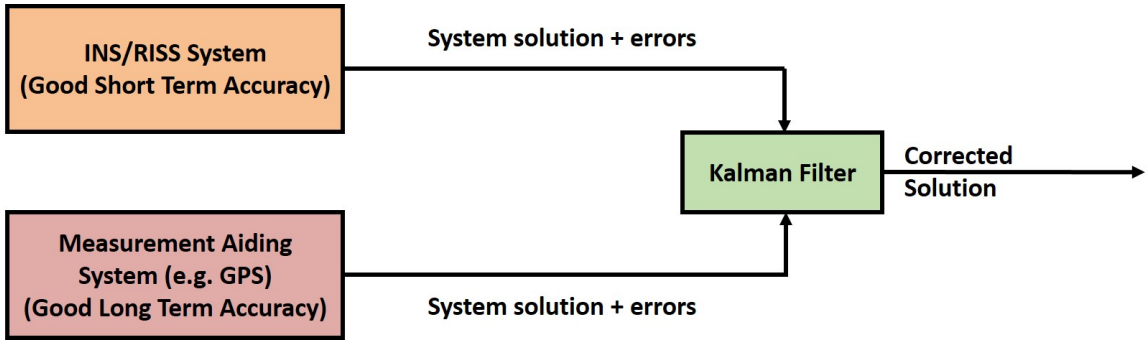

Figure 2.5: KF overview for GPS/RISS integration

2.1.2.2 2D/3D RISS

To reduce both the cost and the accumulation of the aforementioned errors due to the double integration in INS, another system was introduced which is called Reduced Inertial Sensor System (RISS). For 2D navigation, only one gyroscope is required with one odometer responsible to measure the speed assuming that the vehicle is moving in the horizontal plane. On the other hand for 3D navigation, one gyroscope, three accelerometers and one odometer (also known as speedometer) are needed. Errors are reduced because only a single integration of velocity measurement is done to obtain the displacement instead of double integration used in case of accelerometers. However, the error accumulation still exists and thus accuracy cannot be maintained for a long time [8]. Accordingly, RISS will be considered in the following sections instead of INS.

The complimentary characteristics of GPS and RISS support the integration of both to provide more reliable positioning over short and long term. KF is typically used which will be discussed in the next subsection to fuse measurements from both systems.

2.1.3 Integration of GPS/RISS using Kalman Filter

As mentioned earlier, the position provided by the RISS system suffers from error accumulation over time. To limit this, position and velocity from GPS are integrated with RISS. The widely used methods for GPS/RISS integration are estimation techniques such as KF [8]. Figure 2.5 shows an overview for GPS/RISS integration using KF. It is considered to be the optimal estimator of the error states in any system (i.e. RISS) with noisy measurements (GPS) when the error follows a Gaussian distribution. KF can use all the available information of the system including

the initial states, its model and noises as well as the external measurements and errors to estimate the current state. One of the major advantages of KF is that it provides data in real time and models the system dynamics.

The main assumptions in KF are that both the system model and the measurement model should be linear, the errors in the system and the measurements are independent and they should follow white Gaussian distribution. The methodology of KF is considered to be recursive that estimates the current state and uses the noisy measurement as a feedback loop to estimate the next state. The operation of KF consists of two phases, prediction and measurement. In the prediction phase, KF estimates the current state of the system and its accompanied noise covariance using values from the previous time epoch as shown in Eq. 2.1 and 2.2. This is followed by the measurement phase in which KF updates and enhances the previous estimates based on the current external measurements as shown in Eq. 2.3, 2.4 and 2.5. In essence, the final (posterior) state at a certain time epoch is a weighted sum between the measurements and the predicted (prior) states as in Eq. 2.4. Such weighting is done using Kalman gain which is a function of both the states and measurements error covariance matrices as in Eq. 2.3.

Prediction Phase:

$$\delta X_t^- = F_{t,t-1}\delta X_{t-1}^+ + G_{t-1}W_{t-1} \tag{2.1}$$

$$P_t^- = F_{t,t-1}P_{t-1}^+ F_{t,t-1}^T + G_{t-1}Q_{t-1}G_{t-1}^T \tag{2.2}$$

Measurement Phase:

$$K_t = P_t^- H_t^T (H_t P_t^- H_t^T + R_t)^{-1} \tag{2.3}$$

$$\delta X_t^+ = \delta X_t^- + K_t(Z_t - H_t \delta X_t^-) \tag{2.4}$$

$$P_t^+ = P_t^- - K_t H_t P_t^- \tag{2.5}$$

Where:

- δX is the error state vector.
- $(-)$ and $(+)$ are the superscript signs that define the predicted and corrected values, respectively.
- t is the measurement time epoch.
- $F_{t,t-1}$ is the state transition matrix that models the dynamics in the system states each epoch.
- G_{t-1} is the noise distribution matrix.
- W_{t-1} is the process noise vector.
- P_{t-1} is the state error covariance matrix.
- Q_{t-1} is the process noise covariance matrix.
- H_t is the design matrix that expresses the linear relation between the system states and the measurements.
- N is the total number of neighboring vehicles.
- R_t is the measurement noise covariance matrix.
- K_t is the Kalman gain matrix.
- Z_t is the measurement/observation matrix.

As mentioned before, one of the main challenges when using KF is that the system and the measurement models should be linear which is not usually the case in localization such as multilateration. For this reason, before applying KF, the non-linear model should be linearized. Thus instead of modeling the states as positions that have a non-linear relation with the measurements (e.g. distances), linearization is done to represent the states as the errors in the positions. The two methods used for KF linearization are Linearized KF (LKF) referred also as KF and EKF which are based on open-loop and closed-loop realization schemes, respectively. In the open loop approach, there is no feedback from the KF estimates and each filtered solution is calculated without

the need of any feedback corrections. While in the closed loop approach, the filtered solution is used as a feedback in the process to correct the next epochs.

There are two main types of GPS/RISS integration, loosely coupled and tightly coupled. In the loosely coupled, GPS position and velocity are provided first and then they are used as the measurement phase in KF to correct the RISS measurements. This is done by taking the difference between the positions from GPS and RISS to estimate the error that should be added to the RISS solution. The tightly coupled technique uses the raw data from the satellites (e.g. pseudorange measurements) along with the corresponding RISS measurements to provide solution by estimating the error in RISS. The main advantages of loosely coupled is its simplicity however, the measurement update requires the availability of at least four GPS satellites to obtain a position. Whereas, tightly coupled integration provides better accuracy in addition to the ability of providing RISS error corrections with any number of available satellites. Thus, tightly coupled integration can dominate in urban areas but at the expense of increased complexity that incorporates raw data processing at the receiver.

In the upcoming sections, non-cooperative localization techniques introduced in the literature for VANETs are reviewed. The GPS and INS (or RISS) are typically used alongside other systems in the infrastructure of the surrounding environment, this is followed by the main cooperative techniques as well.

2.2 Non-Cooperative Localization Schemes for VANETs

As mentioned previously, the common techniques used in localization are GPS and INS (or RISS). However, the GPS error range is not acceptable in most of the safety applications and also in case of outages and INS cannot survive for a long time because of the error accumulation. For these reasons, many techniques were presented in the literature to enhance the accuracy of the localization by integrating both systems together rather than using each as a standalone system. Integration can be done using estimation methods such as KF, EKF, or other filtering techniques (e.g. particle filter or neural networks). In [14], the GPS raw data along with the corresponding INS measurements of the vehicle are fused together using KF for final position estimation. While in [15], the GPS position of a vehicle is corrected using Differential GPS (DGPS), then this updated position is enhanced by its fusion along with the INS measurements through EKF. The DGPS

concept is based on installing GPS receivers with known locations on the road. These receivers periodically calculate the difference between their known positions and the positions obtained using the current GPS measurements. This difference represents the errors in the current GPS signal and thus will be broadcasted to all nearby vehicles in order to correct the vehicles' GPS measurements based positions given that the errors are correlated between the nearby GPS receivers [2].

Integration can also be accomplished using intelligent techniques such as neural networks in [16] and [17] or fuzzy logic [18]. Hybrid techniques can be also applied as in [19] where filtering is done first to remove the outliers and the noise from the measured data, then neural networks is adopted to enhance the localization accuracy.

In all the above techniques, the accuracy of a combined GPS/INS integration is enhanced compared to a standalone GPS or INS; however, the accuracy is still not acceptable within some applications since these systems are still dependent on two erroneous sources of information (GPS and INS). In addition, the vehicles in urban canyons that suffer from long GPS outages are dependent only on INS. As a solution, anchors with known positions can be deployed on the road to substitute the GPS absence and provide accurate positions to the nearby vehicles through any landmarks (e.g. light poles) [11] or Road Side Units (RSUs)[7] that are compatible with WAVE protocol and commonly used in VANETs.

In [11], a localization method is introduced to estimate the position of a moving vehicle based on the measurements from the ranging techniques: RTT and AoA. By installing RFID tags on landmarks with known positions, the on-board localization unit in the vehicle is able to measure the RTT of the incoming RFID signal to calculate the distance between the landmark, and the vehicle to be localized. Thus, the vehicle is determined to be on the circumference of a circle in which the landmark is the circle's center, and the radius equals the distance measured. Then, this localization unit measures the AoA of the received signal to detect the angle and the exact location on the calculated circumference. The main challenges in using this technique are the short range of RFID, the cost and the complexity of AoA that requires an antenna array.

The authors in [7], propose a scheme based on two installed RSUs, one on each side of the road. The road is divided into two lanes: one directed to the north and the other to the south. The moving vehicle measures its distance from the two RSUs using ToA ranging technique. This results in two circles that intersect at two points (two candidate positions for the vehicle). In the

next time slot, the vehicle remeasures the distances which results in two more candidate positions due to the vehicle's forward movement. By comparing the recent two candidate positions with the previous pair while knowing the road direction, the vehicle can estimate its actual position. This approach is non robust to the errors in the measured distances as it assumes that the two distances will result in two overlapping circles which is not guaranteed.

In [20], the authors introduce an approach to determine the position of a moving vehicle based on LSM where the anchors are the installed RSUs. Distances are measured between the vehicle and the surrounding RSUs using an RTT ranging technique. Then, LSM is applied to select the position that minimizes the sum of the squared residuals.

Proposed by the authors in [21], a vehicle can localize itself based on the calculated velocity from the on-board sensors, the Doppler frequency shift measurements between the vehicle and the installed RSU, using the latter known position. The Doppler shift is used to determine the vehicle to RSU distance. Moreover, the angle between the vehicle and the RSU is calculated using both the on-board sensors and the Doppler shift velocities. Taking these measurements into account, an EKF is then applied to mitigate the effect of multipath and the channel noise on the calculated Doppler frequency shift and velocities; resulting in a self-localized vehicle.

The above localization schemes show good potential in obtaining accurate positions, especially those that depend on integrating both the on-board sensor readings with the vehicle to RSU measurements through estimation techniques such as EKF. However, the main drawback is that RSUs by design have short coverage ranges, in order to avoid interference, so many nodes have to be installed to guarantee full coverage all over the road which will significantly increase the cost. For this reason, cooperative localization is introduced in the literature to increase the localization accuracy where vehicles exchange information between each other and thus each vehicle works as a mobile anchor for the other vehicles.

2.3 Cooperative Localization Schemes for VANETs

In this section, we present a few of the related and recent cooperative localization schemes for VANETs in the literature.

2.3.1 GPS Raw Measurements

There are VANETs localization techniques that aim to enhance the GPS raw measurements using cooperative information as in [22], [23] and [24]. In particular, vehicles with recent and accurate GPS measurements can broadcast their available pseudoranges and Doppler shifts to other vehicles equipped with low-cost and less accurate GPS receivers. Thus, common multipath errors and clock biases between neighboring vehicles can be removed. In addition, GPS correlated measurements can be used to estimate the inter-vehicle distance rather than the typical ranging techniques such as RSS and ToA [25]. These approaches result in highly accurate localization especially with the availability of high-end GPS and integrated navigation systems in smart vehicles that can mitigate the pseudorange errors of the neighboring vehicles. However, they are not applicable in GPS-denied environments where pseudorange measurements are completely unavailable, and their computational complexity and hardware design put a limitation on their implementation in practice. Next we focus on less complex techniques that enhance the GPS position and not the raw data. These techniques will be followed by recent approaches that consider GPS-free environments.

2.3.2 Total Availability of GPS Positions

In [26], it is assumed that each vehicle has different candidate positions from all the available resources: GPS aided with INS in case of outages, Vehicular to Infrastructure (V2I) communication as discussed in Section 2.2 and using Vehicular to Vehicular (V2V) communication which will be introduced in this section. In case of V2I or V2V, the distance is measured using the ToA ranging technique. Then, optimization problem is used to estimate the vehicle location by minimizing the difference between the ToA-based distance and the calculated distance from GPS-based positions. This position is constrained to the range of an RFID. Then, a smart algorithm is introduced next, to ignore some neighbors that either degrades the performance due to inaccurate positions or increases the complexity in high dense environments. Although this technique will lead to a very good accuracy, its main disadvantage is the dependency on the existing infrastructure in the road and also the GPS measurements, where the former increases the cost while the latter has a higher risk of producing poor accuracy in urban areas. Thus, in the literature, methods

tried to enhance the standalone GPS-based position without the dependency on any infrastructure.

In [27], the authors introduced a simple cooperative localization scheme which is based on the weighted centroid concept. The vehicle to be localized receives messages from the neighboring vehicles containing their positions, then it measures the distances to all the surrounding neighbors in its communication range using the RSS as well as the Signal to Interference Noise Ratio (SINR) of each communication link. The centroid based localization assumes that all the neighbors are equidistant from the source, thus given the distance and the SINR that represents the quality of the distance measurement, a weighting value is assigned to each neighboring vehicle. In particular, the nearest neighbor to the vehicle of unknown position and/or the neighbors with higher SINR will be assigned a larger weight compared to the other neighbors. Later, the authors enhanced their work in [28] where they made changes in the weighting value. Specifically, in addition to the distance, the heading of the neighboring vehicle was also considered and the total weighting value was calculated based on fuzzy logic rules and the certainty in the distance was calculated based on the measured SINR. Thus neighboring vehicles' measurements, with higher SINR will have more weighting values compared to the others with low SINR levels. The main challenge is in deriving the fuzzy logic rules that fit all the practical scenarios and ensure accurate localization.

Another technique is introduced in [29] where the distances between the vehicle and its surrounding neighbors are used to enhance the low accuracy GPS position. Such information is shared among all the vehicles. Based on Bayesian inference, each vehicle updates its new position given the inaccurate GPS positions and the measured distances. The new obtained position is further enhanced by using KF that considers the motion model (position, velocity and acceleration) of the vehicle.

In the technique proposed in [30], the GPS position of a vehicle with an unknown position is enhanced using its neighbors' positions (obtained with more accurate GPS) and the inter-vehicle distances. Then this data is fused using KF for final position estimation along with map matching to ensure that both the output location within the road boundaries and the heading agrees with road direction. While in [31], vehicles are localized using multilateration through Particle Filter (PF) of the GPS estimates of the surrounding neighbors fused with the velocity measurements and ToA as the ranging technique. In the PF, weights are assigned to each vehicle which is based on the GPS position and ToA measurements using likelihood estimation. To enhance the accuracy, map

matching is used. The main advantage of PF over KF is that it has flexible weighting according to the constraint of the vehicle position (e.g. candidate positions outside the road boundaries will be assigned zero weight). In addition, PF is not limited to the Gaussian distribution which is the main assumption in KF [32]. However the main disadvantage is the unsustainable complexity compared to the other estimation techniques due to the large number of particles required for such high accuracy [33].

In [34], the authors proposed a localization technique to enhance the position of a vehicle experiencing low GPS accuracy surrounding by vehicles with higher GPS accuracies. The target vehicle calculates the relative distance between it and the surrounded vehicles using one of the ranging techniques. Then, it computes its position using multilateration of the best neighboring vehicles from the GDoP point of view that describes the geometry of the vehicles and their effect on position error. This position is further enhanced by adopting the adaptive EKF using an INS based position.

Authors in [35], proposed a localization technique that enhances the GPS position of the vehicle using neighbors' GPS positions and measurements based on Euclidean distance called the sensing estimate. The main vehicle is equipped with a radar or any other ranging sensor with high accuracy to be able to sense the vehicles in range with negligible error and then determine their positions with error corresponding to the GPS error of the main vehicle. Thus, a sensing polygon of the vehicles in range including the GPS position of the main vehicle is created. Since all the vehicles have low cost GPS, another polygon of positions is created called GPS polygon. The vehicle enhances its position by comparing the center of mass of the two polygons using a minimal weight matching algorithm. The output position of the vehicle is used in the measurement phase of KF for further enhancement.

Similarly, the proposed technique in [36] applied a matching algorithm between locally generated maps. Each vehicle is equipped with a low accuracy GPS receiver and on-board sensors with high-level accuracy that detect the surrounding neighboring vehicles with negligible errors. Thus each vehicle can produce its local map that contains its own position measured from the low accuracy GPS and the relative positions of the detected vehicles using the ranging sensors. Each vehicle broadcasts its own map to the surroundings. In each map, all the positions have almost the same GPS error thus each vehicle's position in the map was considered a translated image from the

correct position. The similarities between the maps are evaluated based on a topology matching method. Kalman filter is used to fuse these data.

In [37], a localization scheme is introduced using CFO based on the Doppler shift calculation to estimate the inter-vehicle distances for enhancing the GPS position of a given vehicle. The vehicle fuses its GPS position and velocity with those of the neighbors along with the Doppler shift based distance using EKF. The Doppler shift is used as a ranging technique instead of the common radio ranging techniques RSS, ToA and TDoA because it is less affected by the environmental conditions as multipath and fading. However, the neighbors should be traveling in the opposite direction compared to the source vehicle as the Doppler shift to be identified should be of relatively high value which is reflected by the relative motion and this will not be the case if the vehicles are traveling in the same direction or at low velocities.

In each of the above techniques, it was assumed that all the vehicles have acceptable GPS position estimates. Thus, by using the corresponding localization schemes, the positions of the vehicles are corrected leading to accuracy enhancement. Since this is not usually the case as the GPS positions may suffer from multipath problems which may cause an error in the position estimate and thus, decrease the accuracy. For this reason, the below two implemented algorithms were introduced to overcome the multipath problems of GPS.

In [38], the technique called Inter-Vehicle Communication Assisted Localization (IVCAL) is introduced, which can be used in areas with GPS availability but with low accuracy position as its signal suffers from excessive multipath effect. In this technique, each vehicle can obtain its position using INS readings and then correct it using GPS through KF fusion taking into consideration the error in GPS receiver and INS measurements while assuming no multipath effect. The vehicle then checks whether the obtained position from KF is experiencing multipath or not and thus, each vehicle will have uncertainty evaluation that reflects the confidence in the obtained position. This metric is calculated as the difference between the position estimated from KF and the GPS position using neural networks. The vehicle with low multipath or high certainty can be used as a location anchor to enhance the location for the other vehicles suffering from low certainty. Accordingly, in case of multipath, the position can be further enhanced by applying LSM to minimize the difference between the measured distance through ranging techniques and the calculated distance between the inaccurate position of the vehicle to be localized and the best three neighbor-

ing vehicles. The uncertainty value of the vehicle to be localized will be updated using the worst uncertainty among the selected anchors. In case of fewer than three accurate anchors' positions, the position of the vehicle is set to be the one obtained from KF.

Authors extend their work in the IVCAL algorithm in [39], by introducing two methods to solve the LSM optimization problem. The first method is the unconstrained scheme in which all the neighboring vehicles in range are considered to be anchors and not only the best three. This is used to overcome the problem of poor geometry alignment of the neighbors (e.g. collinear). The second method is the constrained weighting scheme. In this scheme, the three best anchors chosen to solve the LSM are used to enhance the localization. However, the uncertainty value of its location is used as a confidence boundary to reflect its weight in the localization.

In all the above techniques, it was assumed that all the vehicles in the area are equipped with GPS and the necessary satellite's signal is not blocked which is not the case in the practical scenarios, so the three techniques from the literature described in Subsection 2.3.3 assume that only some of the vehicles are having GPS estimate positions.

2.3.3 Environments with partial GPS Access

The scope of the technique in [40] is to enhance the localization accuracy of the vehicles equipped with GPS and also localize the non-equipped vehicles while communicating with the equipped ones. RFID tags are installed on the landmarks along the road with known positions while both RF tags and readers are installed in the vehicles. The RFIDs on landmarks are used to localize non-GPS vehicles within their coverage range. Accordingly, these GPS vehicles are considered to be mobile references that localize and enhance localization accuracy of the first hop nearby GPS vehicles; and for non-GPS vehicles out of range of stationary RFIDs, they are localized through the accurately localized GPS vehicles. This technique can be summarized as follows:

- For GPS vehicles: Once the vehicle travels in the vicinity of a landmark RFID tag, the vehicle calculates its accurate position when it receives the known position of the landmark in addition to both the distance and orientation (angle). This vehicle can also calculates its another candidate position using the GPS whose error is corrected using the RFID-based

position. This vehicle then works as a reference that broadcasts the GPS error to the first tier neighbors. These neighbors can then compensate their GPS position errors using the broadcasted values.

- For non-GPS vehicles: These vehicles also calculate their accurate positions using the RFID landmarks in range as done for the GPS vehicles. For those outside the coverage of the landmark, they use the GPS equipped vehicles in their communication range taking into account both the speed and orientation.

The objective in [41] is to enhance the accuracy of GPS equipped vehicles, and localize other vehicles not equipped with GPS. To enhance the location accuracy of each GPS equipped vehicle, the velocity measurement from on-board sensors as well as the intervehicle distance are used to apply a multilateration technique where the surrounding GPS equipped vehicles are used as anchors. For localizing non-GPS equipped vehicles, each surrounding vehicle provides a candidate position at different time epochs for the vehicle to be localized. A weighting value is then assigned to each candidate position based on its freshness[1] to use all these position candidates in the multilateration. Moreover, each vehicle can have different position estimates with different likelihood values measured independently using the surrounding vehicles. The true position is nearer then to the one with higher likelihood.

In [42], the authors proposed a localization technique where some vehicles are equipped with GPS. The scheme is based on a grid approach which assesses some geometric relation patterns between the vehicles. The neighbors selected in the localization process are the vehicles with good GPS positions and at a distance from the vehicle to be localized smaller than a certain threshold. The target vehicle to be localized can calculate the distances between itself and the neighboring vehicles using RSS even if the latter have unknown positions. The algorithm solves the problem of less than three surrounding neighbors with known positions or collinearity problem in case of three neighbors by mapping the target vehicle and its neighbors into a map and calculates the unknown position using proposed geometric patterns G2-1 or G2-2. The first number is the number of neighbors with known positions surrounding the target vehicle, while the second number represents the number of neighbors with known positions referred to here as the known

[1] Recent time of position measurement

neighbor that surrounds a neighbor to the target with unknown position referred to here as the unknown neighbor. This means that this algorithm can localize a vehicle if it is surrounded by at least two vehicles with known positions and one vehicle with unknown position in the condition that the latter vehicle has at least one neighbor with known position. This is done firstly by dividing the map into small grids and checking all the possible locations of the target vehicle using the distances to its two known neighbors after ignoring the locations outside the roads. Then do the same for the unknown neighbor using the one or two known neighbors according to G2-1 or G2-2 respectively. The correct location of the target that satisfies the known distance between it and the unknown neighbor is chosen. The main drawbacks are that the geometric patterns proposed should be satisfied in the real world and the accuracy of localization depends on the size of grid and the complexity.

Sometimes moving vehicles equipped with GPS receivers may only have good GPS position estimates before they reach crowded areas with high buildings. Thus to address this situation which usually happens in downtown canyons, a dead reckoning scheme which is introduced before is used but the main drawback is that its error deviates and increases over time and this will be a major problem if the GPS outage lasts for a long time. So to solve this issue, some techniques based on cooperative localization are proposed in the literature as reviewed below.

2.3.4 GPS-Free Environments

In [43], the Cooperative Inertial Navigation (CIN) technique is introduced to enhance the accuracy of INS standalone. In CIN, the vehicles share their IMU measurements alongside their INS-based positions with all the vehicles traveling in the opposite direction and then fuse these data with CFO to estimate the position.

In [44], an algorithm VLOCI, is introduced where every vehicle has the initial position measured using GPS and has a set of estimated positions calculated from the surrounding neighbors. Each estimated position is equal to the position of the neighbor which is assumed to be correct plus or minus the inter-vehicle distance calculated using ToA or RSS. The intervehicle distance should be added to the neighbor's position or subtracted since all the vehicles are moving in the same lane and direction, this means that the neighbor might be behind or in front of the vehicle to be localized. The final position is calculated using the weighted average function by assigning

each position a weighting value. Since the distance is calculated using the ranging techniques mentioned previously, the accuracy of the distance is lower when the neighbors that are further away. Thus, the weighting value is inversely proportional to the calculated distance.

Then in [45], the authors extended their work in VLOCI to the VLOCI2 algorithm by adding a smart lane algorithm that takes into consideration a multi-laned road scenario. To avoid vehicles from drifting and to maintain the distances at a good accuracy since all these positions suffer from errors, they considered two scenarios: If the final position is in the same lane as the GPS position, then the final x position is updated to be the midpoint between them, and the final y position is the lane center. On the other hand if the final position is on a different lane than the GPS position, the updated position will be the midpoint of these two positions.

Moreover in [46], the authors enhanced the work done in VLOCI/VLOCI2 by updating the scheme to provide good localization accuracy considering multiple lanes. To know the position estimate for each vehicle, AoA is measured in addition to the ranging techniques mentioned in the VLOCI algorithm to determine the location. Furthermore as in the VLOCI technique, the final position is calculated using the weighted average function of the position estimates but this position is further fused along with GPS position using EKF and/or PF for an updated position. The position accuracy is enhanced by assigning to each position estimated a weighting value proportional to the belief of the current position of the vehicle using EKF and/or PF. AoA technique is not considered as a good solution for localization since it is highly affected by the multipath that results in high localization error. Even if an antenna array is used in the vehicle to limit the error, it is considered to be an expensive solution [5].

A centralized RSS cooperative approach for a cluster of n vehicles was introduced in [47] and [48]. Each vehicle measures its distance with the neighboring $(n-1)$ vehicles based on RSS. These neighbors also report their velocities from on-board sensors. Then, all this information is collected by the n vehicles and used to compute their positions using EKF. Additionally map matching is used to ensure that the localization is done within the permitted boundaries. In particular, the EKF uses the total $n \times (n-1)$ measurements within the cluster to 1) predict the states with the on-board velocities and 2) correct them using the RSS based distances. The main focus was to mitigate the error in the RSS based distances and their effect on the accuracy of the cooperative scheme. Nevertheless, the computational complexity cannot be easily handled for real time and

safety applications. In the next chapter, the overview of the preliminaries of the system and of the implemented distributed cooperative scheme is introduced. Our proposed distributed scheme is less complex that adopts RTT instead of RSS while EKF handles the errors in the sensors and the neighbors' positions.

Chapter 3

System Overview

3.1 Preliminaries and Design Details

As mentioned earlier, the typical technique used in localization is GPS as most vehicles nowadays are equipped with GPS receivers. However, when the vehicles travel in urban or dense areas, the GPS fails to reach its goal as it suffers from successive outages due to high rise buildings multipath or complete GPS blockage experienced in tunnels. For these reasons, INS/RISS is used to replace GPS in case of several outages in urban areas in the hope that the outage will not last for a long time. The assumption of a short outage duration might not hold practically, thus cooperative localization between vehicles using trilateration/multilateration techniques is introduced in the literature besides INS to assist GPS whenever it is unavailable for a specific number of vehicles.

Multilateration techniques can be used to determine the unknown 2D position of a given vehicle by knowing the positions of at least three surrounding neighbors along with the inter-vehicle distance between the unknown position and each neighbor. In the multilateration equation shown in Eq. 3.1, the unknown position, the neighbors' positions and the measured inter-vehicle distance using a ranging technique are denoted as (x, y), $(x^{(n)}, y^{(n)})$ and $d_m^{(n)}$, respectively where n is the neighbor index. x and y correspond to the positions in rectangular (Cartesian) coordinates in the Earth-Centered Earth-Fixed (ECEF) frame. The left hand side in Eq. 3.1 which is a function of both the vehicle's unknown position and the neighbor's position is known as the Euclidean distance and it is referred here in our work to the estimated distance $d_{est}^{(n)}$.

$$\sqrt{(x^{(n)} - x)^2 + (y^{(n)} - y)^2} = d_m^{(n)} \tag{3.1}$$

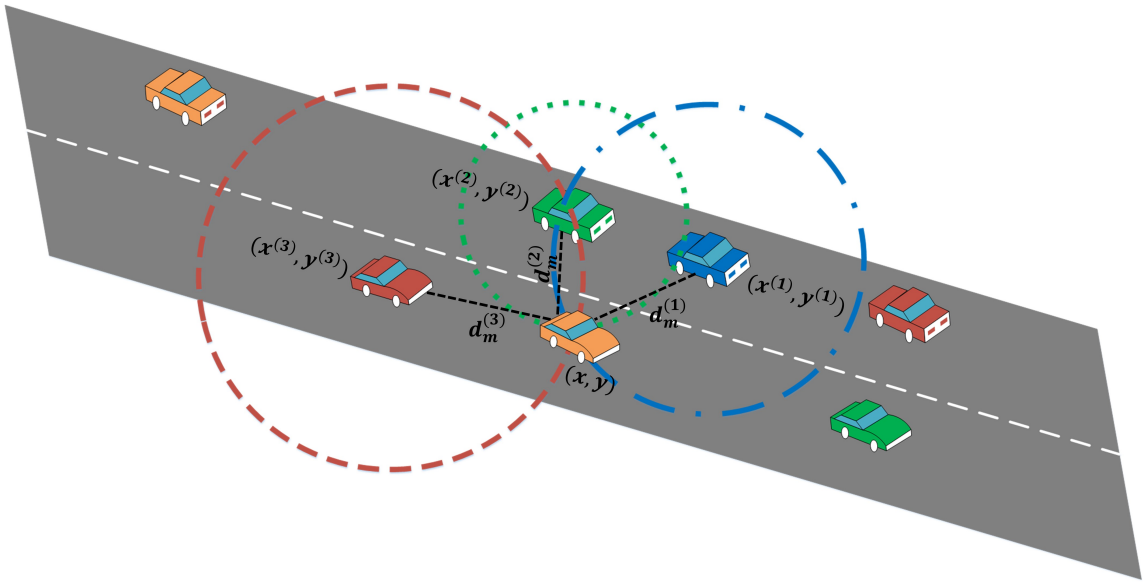

Figure 3.1: Example of trilateration in VANETs

By simultaneously solving Eq. 3.1 given three neighbors for example ($n \in \{1,2,3\}$), the unknown 2D position is obtained as shown in Fig. 3.1. In particular, solving the three equations corresponds to finding the intersection point of the three circles which is the unknown position in our case. However, such an intersection is not guaranteed or does not represent the correct position if the positions of the neighbors and/or the measured inter-vehicle distances suffer from errors. Accordingly, the correct position is determined as the one that minimizes the difference between the squared measured and the squared estimated distances as depicted in Eq. 3.2.

$$min_{x,y} || \sum_{n \varepsilon N} (d_{est}^{(n)} - d_m^{(n)})^2 || \tag{3.2}$$

An example of a commonly used method to solve the above equation as mentioned earlier is LSM. The main disadvantage of LSM is that it does not take into consideration the system dynamics which is represented by the change in both the neighbor's position and the inter-vehicle distances over the time. This issue is addressed when using KF which is considered to be the best linear estimator [8] that takes into account the previous states within a real time complexity. Thus a localization technique that relies on integrating RISS and a cooperative technique using EKF is proposed in this thesis to obtain the position of a given vehicle in a GPS-free environment. Below are the assumptions used in this work:

- All vehicles have initial positions only in the first time epoch obtained either from GPS or any other localization system as in [48]. Practically, most of the vehicles are equipped nowadays with GPS that might be able to obtain open sky access at road intersections. Then, these vehicles move in an urban area where GPS suffers from several outages or complete blockage.

- Vehicles are equipped with DSRC transceivers, thus each vehicle to be localized can communicate with its neighboring vehicles and exchange information between each other in the communication range via IEEE 802.11p protocol. The neighbors in range are the vehicles that are able to receive messages from the vehicle to be localized with power greater than minimum threshold level (referred as receiver's sensitivity).

- Each vehicle is able to measure the distance to its neighbors using one of the ranging techniques [5]. Round Trip Time (RTT) is chosen as it does not require synchronization since the same vehicle will be calculating the difference between the time of transmission and reception. Moreover, RTT is proven to be robust to the channel and synchronization errors for measuring inter-vehicle distances [11]. Thus, no error was introduced to the RTT as the delay offset that is generated from the processing can be calibrated and thus multipath and fading effects can be easily mitigated [20].

- The vehicles are also equipped with inertial navigation sensors to assist in the localization and enhance the accuracy. Such sensors exist in the current vehicles and their information can be reported and extracted from the on-board unit. The 2D RISS applied here comprises of odometers that measure the horizontal speed and, the gyroscope that determines the heading of the vehicle. Unlike previous schemes, our technique updates the neighbors' locations through their on-board sensors/RISS readings prior to using them in localization. We define the following two system entities:

    1. *Sender (s)* is the vehicle to be localized that sends messages to the surrounding vehicles acquiring information for localization.

    2. *Neighbor (n)* is the vehicle within the communication range of the sender vehicle that receives the messages and then replies back to the sender with its information (location

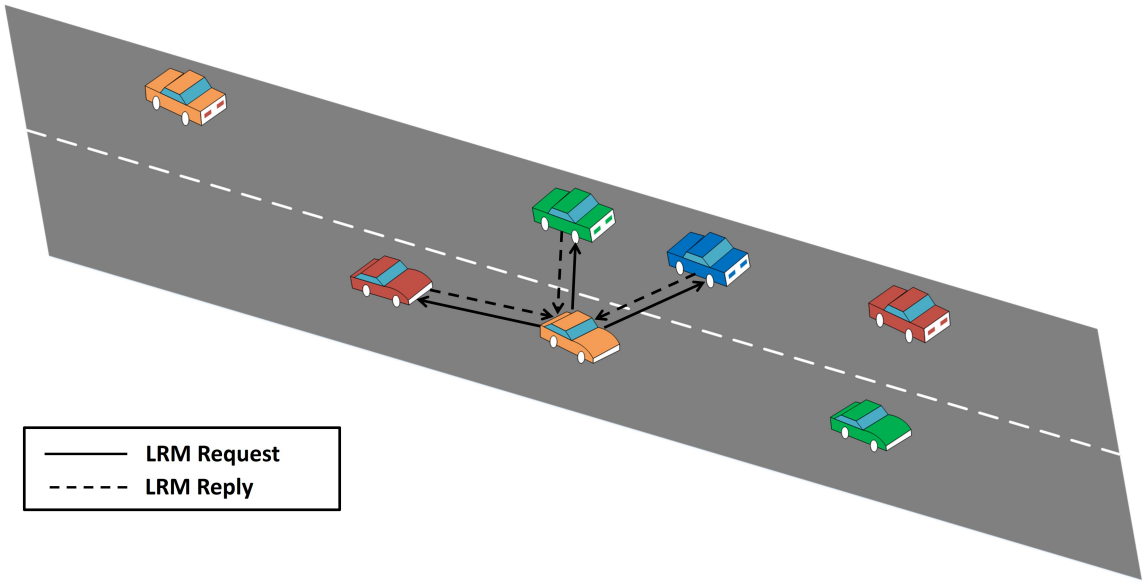

Figure 3.2: Two-lane road simple cooperative scenario

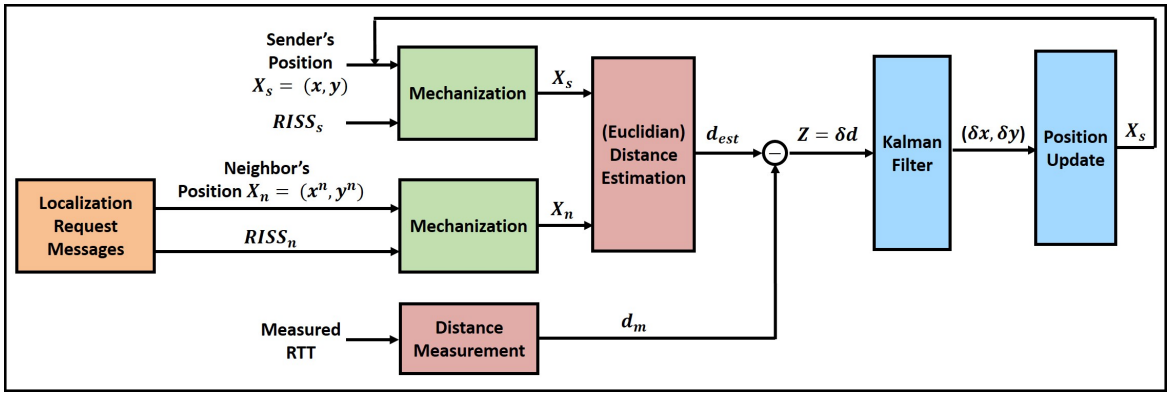

Figure 3.3: Block diagram of the proposed cooperative scheme

and RISS measurements).

A simple scenario of a two-lane road where the sender vehicle communicates with its neighbors in range is shown in Fig. 3.2. The sender requests information *(solid lines)* from the neighbors which in turn will reply back *(dashed lines)* with the demanded information.

3.2 Cooperative Scheme Overview

This section presents the proposed scheme overview for the vehicle to be localized. In Fig. 3.3, the main blocks of our cooperative system are shown and can be described briefly in the following seven main steps:

1. The sender vehicle requiring localization triggers the system by broadcasting a Location Request Message (LRM) for collecting neighbors' navigation information in range (both location and RISS measurements) needed in the localization.

2. The received outdated neighbors' positions are corrected at the sender by applying RISS mechanization using their reported sensor measurements. The neighbors' positions are outdated from the second time epoch as there is no GPS updates. These outdated positions will affect the accuracy of the position of the vehicle to be localized if applying the proposed cooperative localization technique in this time epoch. For this reason, mechanization is done to ensure that the neighbors are having updated positions before applying the cooperative scheme.

3. RTT is calculated at the sender and used to measure the actual distance d_m between the sender vehicle and the neighbor which responded to the broadcasted messages.

4. The sender vehicle updates its position using the RISS mechanization. If the outdated sender position is used when calculating the Euclidean distance between it and its neighbor, this distance will be subjected to high error and will not reflect the actual distance between them. Thus, mechanization is applied to the sender to have an updated position of the vehicle to be localized.

5. The Euclidean distance d_{est} is a function of both the sender's and the neighbors' positions. However, since these two positions are calculated based on RISS, they suffer from the inaccuracies of the mechanization process and the errors associated with both the sensors and the previous positions. Thus, the measured distance d_m using the ranging technique is adopted to correct the estimated distance and calculate a final accurate position of the sender vehicle.

6. Linearized EKF technique uses the error difference between d_{est} and d_m to estimate the error in x and y positions of the sender vehicle. This reflects the error in d_{est} while the error in d_m is assumed to be negligible as a fact of applying RTT.

7. The estimated x and y errors are then used to update the sender's position for future localization.

Chapter 4

Integrated Cooperative Localization using EKF

In this chapter, the proposed integrated cooperative localization scheme will be discussed in detail. Figure 4.1 shows a flow chart illustrating the methodology. The main blocks of the system which were briefly introduced in Section 3.2 will be described in the following sections. The blocks implement the four main stages below:

1. LRM that contains all the neighbors' information requested by the sender vehicle.
2. Mechanization that updates the sender and the neighbors' positions for better localization accuracy.
3. Inter-vehicle distance measurement d_m using ranging technique and Euclidean distance computation d_{est} using the vehicles' positions which are needed in the localization process.
4. EKF that uses the difference between d_m and d_{est} from the previous input to measure the error that should be added to the sender location for final position update.

4.1 Exchange Localization Request Messages (LRM)

Each sender vehicle, to be localized, requests its neighbors' navigation information (position, heading and speed) through broadcasting messages. The broadcast message contains both the ID of the vehicle to be localized denoted as sender ID and time of transmission T_{TX}. All messages are broadcasted in the DSRC range every τ seconds. The neighboring vehicle in the communication range that receives the signal containing the message with power greater than its sensitivity power level $\hat{P}$ will add its navigation information (latest positions, current heading and current odometer reading) to this message and then rebroadcast it. The latest position of the neigh-

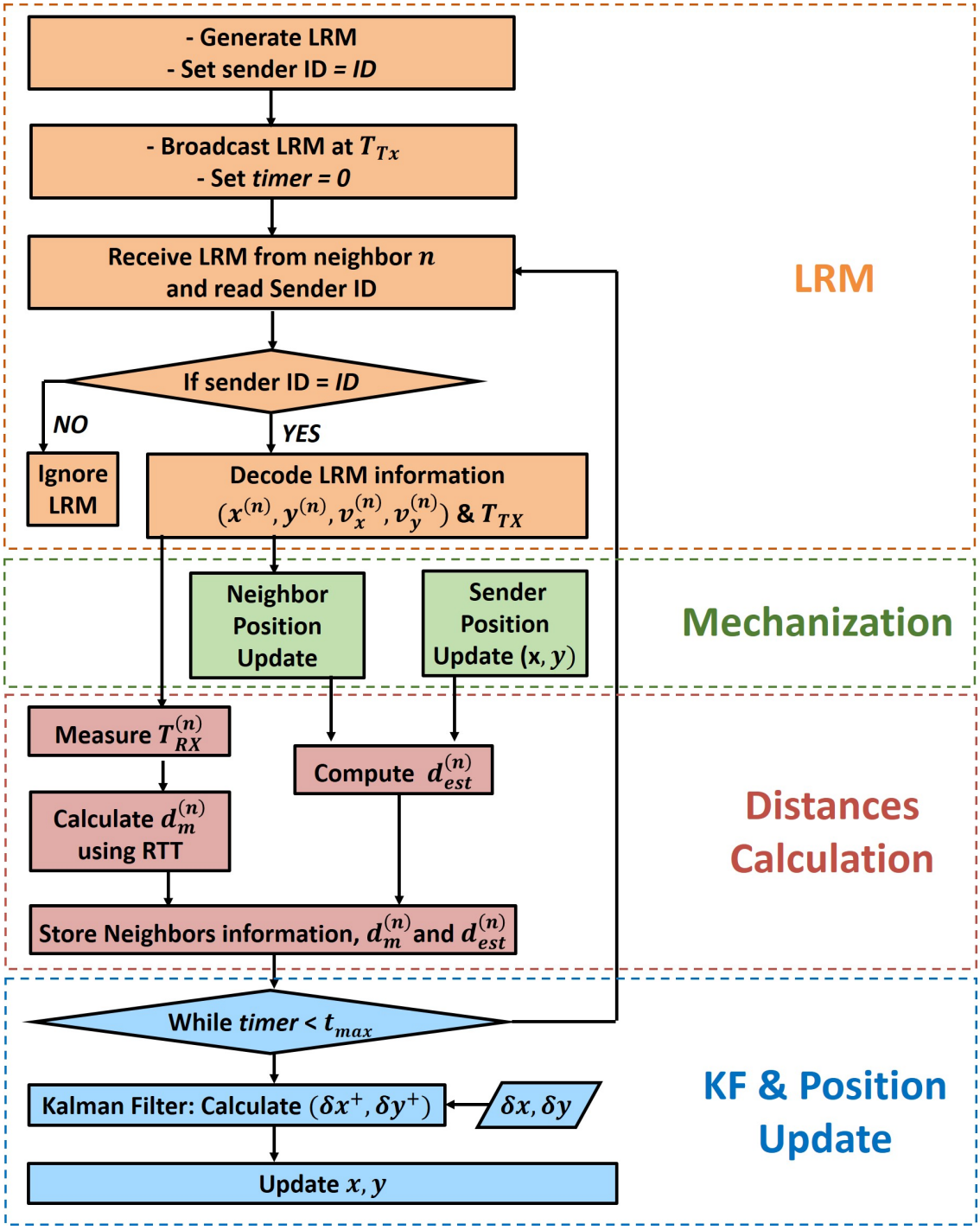

Figure 4.1: Flow chart of the proposed cooperative scheme

bor might be outdated by the time it is reported and thus it is accompanied with the above inertial sensor readings for its correction.

Once the vehicle to be localized receives back the neighbor's message, it checks whether

the received message is a reply to its own broadcasted LRM or not. This is done by comparing its ID with the one appended in the reply message of the sender ID. If the IDs are identical, the message is decoded, otherwise it is ignored. The sender measures the time of reception of the LRM T_{RX}. The LRM message contains the following information:

- Neighbor's position denoted by its coordinates $x^{(n)}$ and $y^{(n)}$ where n is the neighbor's index. This position is the last updated available one at the neighbor which might be outdated from the current time of LRM reception. Accordingly neighbor's velocity and heading are also broadcasted.
- Neighbor's velocities in both x and y directions, respectively denoted as $v_x^{(n)}$and $v_y^{(n)}$, obtained from the odometer readings. Similarly, the neighbor's heading denoted as $A^{(n)}$ is measured using the gyroscope.
- Time of transmission of LRM T_{TX} is used to measure the actual distance to the neighbor $d_m^{(n)}$ using RTT.

The above neighbor's information is used to update the received neighbor's position using RISS which will be used afterwards in the computation of the Euclidean distance $d_{est}^{(n)}$ between the vehicle to be localized and the neighbor n.

4.2 2D Reduced Inertial Sensor System (RISS) Mechanization

As mentioned earlier, the neighbor reports in the LRM its last updated position which may be outdated at the time of the localization of the sender vehicle. This is because in our proposed cooperative scheme, it was assumed that all vehicles travel in urban areas where there is no GPS location updates. RISS [8] is used instead to update the neighbors' positions as well as the position of the vehicle to be localized. 2D RISS was considered as it was assumed that the neighboring vehicles are nearly on the same heights and thus 2D Euclidean distance only is needed. This is done at lower cost with reduced error compared to the full INS as the former consists of only two sensors, the odometer and the gyroscope as mentioned previously in Subsection 2.1.2.2.

The gyroscope is used to determine the vehicle's orientation in the horizontal plane (the azimuth angle). Typically, the gyroscope measurements are associated with both the earth's rota-

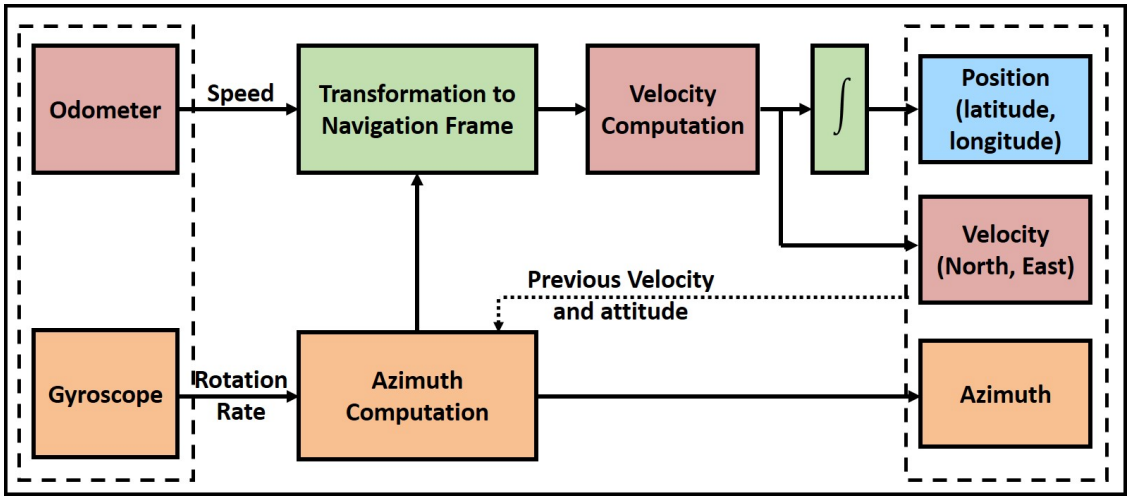

Figure 4.2: 2D RISS mechanization block diagram overview

tion rate along its vertical axis $w^e sin(\phi)$ and the change of the vehicle's orientation in the local level frame relative to the earth $\frac{V_E tan(\phi)}{R_N+h}$ in addition to the angular velocity w_z. Thus the rate of change of the azimuth angle $\dot{A}$ is expressed in Eq. 4.1. The computed $\dot{A}$ is used to obtain the azimuth angle A which is used along with the vehicle speed measured using the odometer to determine V_E and V_N assuming that the vehicle is moving only in the horizontal plane. Then, V_E and V_N are further used to obtain the rate of change in the latitude $\dot{\phi}$ and the longitude $\dot{\lambda}$ while considering transformation from Cartesian to curvilinear coordinates as shown in Eq. 4.3. $\dot{\phi}$ and $\dot{\lambda}$ are then integrated over the sampling interval for updated latitude ϕ and longitude λ positions. The overview of the block diagrams of the 2D RISS mechanization is shown in Fig. 4.2.

In our simulated work for simplicity, Eq. 4.4 is considered rather than Eq. 4.1 since the two terms $w^e sin(\phi)$ and $\frac{V_E tan(\phi)}{R_N+h}$ are negligible compared to w_z over a short duration of time. Furthermore, the information from the gyroscope in Eq. 4.4 and odometer sensors are used to compute the velocities in the east V_E and north directions V_N shown in Eq. 4.2. Moreover, these velocities are directly integrated to calculate the east and north displacements which in turn are used to compute the E and N positions corresponding to x and y positions, respectively [49].

$$\dot{A} = w_z - w^e sin(\phi) - \frac{V_E tan(\phi)}{R_N + h} \tag{4.1}$$

$$\begin{pmatrix} V_E \\ V_N \end{pmatrix} = \begin{pmatrix} V_{od} \times sin(A_t) \\ V_{od} \times cos(A_t) \end{pmatrix} \tag{4.2}$$

$$\dot{r} = \begin{pmatrix} \dot{\phi} \\ \dot{\lambda} \end{pmatrix} = \begin{pmatrix} 0 & \frac{1}{R_M+h} \\ \frac{1}{(R_N+h)\times cos(\phi)} & 0 \end{pmatrix} \begin{pmatrix} V_E \\ V_N \end{pmatrix} \tag{4.3}$$

$$\dot{A} = w_z \tag{4.4}$$

Where:

- $\dot{A}$ is the rate of change in azimuth (heading angle).
- w_z is the angular velocity measured by the gyroscope.
- w^e is the earth rotation rate.
- ϕ is the latitude.
- $w^e sin(\phi)$ is the vertical component of the earth rotation rate.
- V_E is the east velocity.
- R_N is the normal radius.
- h is the altitude.
- $V_E tan(\phi)$ is the orientation change of the local level frame with respect to the earth.
- V_{od} is the vehicle's horizontal speed measured by the odometer.
- A_t is the current azimuth (heading angle) of the vehicle.
- V_N is the north velocity.
- $\dot{\phi}$ and $\dot{\lambda}$ are the rate of change in latitude and longitude respectively.
- R_M is the meridian radius.

The error in the simulated odometer and the gyroscope follow the Gaussian distribution. For the simulated gyroscope, the error introduced is the Angular Random Walk (ARW) as it was

assumed that the deterministic component (bias) of the error is perfectly compensated before hand [8]. After updating both the sender and the neighbors' positions using RISS, inter-vehicle distance is calculated using the ranging technique as well as the Euclidean model.

4.3 Inter-Vehicle Distance Calculation

Based on the collected information, localization techniques such as multilateration cannot be applied to obtain an updated position for the vehicle to be localized because of the associated errors in these measurements as mentioned in Section 3.1. Instead, linearized Kalman filter model such as EKF can be used to obtain an accurate position update [8]. EKF works with errors in both: distances and positions (rather than the actual distances and positions) to reserve its linearity such that it relates the error in the unknown position to the error between the two distances (i.e. the one measured using RTT and the Euclidean one estimated using the vehicles' positions) to be compensated for final position update. In the following subsections, the two values of distances between the sender vehicle and each neighbor are described in further detail.

4.3.1 Euclidean Distance Estimation d_{est}

The first distance is denoted as $d_{est}^{(n)}$ and calculated based on the vehicles' latest positions as depicted in Eq. 4.5. It is the Euclidean distance between the RISS based updated position of the sender vehicle and its neighbor n. Thus, this distance is subjected to errors that are associated with the vehicles' positions due to the odometer, gyroscope and the vehicles' previous positions errors.

$$d_{est}^{(n)} = \sqrt{(x^{(n)} - x)^2 + (y^{(n)} - y)^2} + e \tag{4.5}$$

Where:

- $x^{(n)}$ and $y^{(n)}$ is the RISS mechanization based updated position of neighbor n.
- x and y is the latest position of the sender vehicle (after RISS mechanization).
- e is a random variable that models the associated errors in the vehicles' positions.

4.3.2 Inter-Vehicle Distance Measurement d_m

The second distance denoted as $d_m^{(n)}$ is calculated using the ranging technique RTT as shown in Eq. 4.6 and Eq. 4.7 using the time difference between the transmission and the reception of the LRM at the sender and denoted as T_{TX} and T_{RX}, respectively . No error was introduced to the RTT as the delay offset that is generated from the processing can be calibrated and thus multipath and fading effects are mitigated as mentioned earlier [20]. Thus, $d_m^{(n)}$ reflects the actual distance between the sender vehicle and the neighbor n.

$$RTT^{(n)} = T_{RX}^{(n)} - T_{TX} \tag{4.6}$$

$$d_m^{(n)} = \frac{c \times RTT^{(n)}}{2} \tag{4.7}$$

Where:

- $RTT^{(n)}$ is the duration between the transmission of LRM and reply's reception from its neighbor n.
- c is the constant speed of light.

As discussed earlier, the calculated Euclidean distance in Subsection 4.3.1 has many sources of errors and noise associated with the measurements. As such, KF/EKF which is described in Subsection 2.1.3 is the best linear estimator as the error in sensor measurements and vehicles' positions follow a Gaussian distribution [8]. EKF used in this research estimates the errors in both the x and y positions of the vehicle to be localized for a final position update.

4.4 Kalman Filter and Position Update

In this section, we first review the existing GPS/RISS non cooperative integration typically done using KF. Next, this model is extended to GPS-free environments in which cooperative information is used with the RISS measurements through EKF.

4.4.1 Conventional Non Cooperative GPS/RISS Integration using Kalman Filter (KF)

KF is typically used to integrate RISS with GPS measurements for a final position estimation as mentioned in Subsection 2.1.3. An example is implemented in [50] where KF is used to estimate the error state vector δX that includes the errors associated with the RISS measurements using the GPS updates. δX consists of the error in the latitude and longitude positions, error in the east and the north velocities, error in the azimuth and the random errors associated with the odometer and gyroscope as depicted in Eq. 4.8. Moreover, Eq. 4.9, Eq. 4.10 and Eq. 4.12 represent the rate of change of the errors over the time as a function of the previous error states. Such equations model the change of the states over time due to both the dynamics of the system and the associated errors in RISS.

$$\delta X_t = \begin{pmatrix} \delta\phi & \delta\lambda & \delta V_E & \delta V_N & \delta A & \delta a_{od} & \delta w_z \end{pmatrix}^T \tag{4.8}$$

Prediction Phase:

$$\begin{pmatrix} \dot{\delta\phi} \\ \dot{\delta\lambda} \end{pmatrix} = \begin{pmatrix} 0 & \frac{1}{R_M+h} \\ \frac{1}{(R_N+h)\times cos(\phi)} & 0 \end{pmatrix} \begin{pmatrix} \delta V_E \\ \delta V_N \end{pmatrix} \tag{4.9}$$

$$\begin{pmatrix} \delta\dot{V}_E \\ \delta\dot{V}_N \end{pmatrix} = \begin{pmatrix} sin(A) & a_{od} \times cos(A) \\ cos(A) & -a_{od} \times sin(A) \end{pmatrix} \begin{pmatrix} \delta a_{od} \\ \delta A \end{pmatrix} \tag{4.10}$$

Where:

- $\delta\phi$, $\delta\lambda$ is the error in the latitude and longitude positions, respectively.
- δV_E, δV_N is the error in the east and the north velocities, respectively.
- δA is the error in the azimuth of the vehicle.
- δa_{od} is the residual random error associated with the odometer driven acceleration.

The rate of change in the azimuth error $\dot{\delta A}$ is ignored while assuming no sudden changes in the vehicle direction and thus $\dot{\delta A}$ is directly equal to the angular velocity error of the gyroscope as in Eq. 4.11. Therefore the error model of odometer and gyroscope can be written as in 4.12.

$$\dot{\delta A} = \delta w_z \tag{4.11}$$

$$\begin{pmatrix} \dot{\delta a_{od}} \\ \dot{\delta w_z} \end{pmatrix} = \begin{pmatrix} -\gamma_{od} & 0 \\ 0 & -\beta_z \end{pmatrix} \begin{pmatrix} \delta a_{od} \\ \delta w_z \end{pmatrix} + \begin{pmatrix} \sqrt{2\gamma_{od}\sigma_{od}^2} \\ \sqrt{2\beta_z\sigma_z^2} \end{pmatrix} w(t) \tag{4.12}$$

Where:

- δw_z is the residual random error in the angular velocity measured by the gyroscope.
- $\dot{\delta\phi}$, $\dot{\delta\lambda}$ is the error's rate of change in ϕ and λ positions of the RISS measurement, respectively.
- $\dot{\delta V_E}$, $\dot{\delta V_N}$ is the error's rate of change in V_E and V_N of the RISS measurement, respectively.
- $\dot{\delta A}$ is the error's rate of change in the vehicle's azimuth.
- $\dot{\delta a_{od}}$ is the error's rate of change associated with the odometer's driven acceleration.
- γ_{od}, σ_{od}^2 is the correlation time reciprocal and the variance of the random process associated with the odometer driven acceleration, respectively.
- β_z, σ_z^2 is the correlation time reciprocal and the variance of the random process associated with the gyroscope measurement, respectively.
- $w(t)$ is a Gaussian random noise with unity variance.

The above Eq. 4.9, 4.10 and 4.12 are used to construct the state transition matrix F and the noise distribution matrix G in order to calculate the state values δX_t using the previous states δX_{t-1} according to Eq. 2.1.

$$F_{t,t-1} = I + F\Delta T \tag{4.13}$$

Where ΔT is the duration of time epoch.

$$F = \begin{pmatrix} 0 & 0 & 0 & \frac{1}{R_M+h} & 0 & 0 & 0 \\ 0 & 0 & \frac{1}{(R_N+h)\times cos(\phi)} & 0 & 0 & 0 & 0 \\ 0 & 0 & 0 & 0 & a_{od} \times cos(A) & sin(A) & 0 \\ 0 & 0 & 0 & 0 & -a_{od} \times sin(A) & cos(A) & 0 \\ 0 & 0 & 0 & 0 & 0 & 0 & 1 \\ 0 & 0 & 0 & 0 & 0 & -\gamma_{od} & 0 \\ 0 & 0 & 0 & 0 & 0 & 0 & -\beta_z \end{pmatrix} \tag{4.14}$$

$$G_{t-1} = G\Delta T \tag{4.15}$$

$$G = \begin{pmatrix} 0 & 0 & 0 & 0 & 0 & \sqrt{2\gamma_{od}\sigma_{od}^2} & \sqrt{2\beta_z\sigma_z^2} \end{pmatrix}^T \tag{4.16}$$

Measurement Phase:

The design matrix H is then used to relate the predicted error states δX and the measurement vector Z. Moreover, due to the independence between the errors in the measurements, the measurement noise covariance matrix R is a diagonal matrix consisting of the GPS associated error variances.

$$H_t = \begin{pmatrix} 1 & 0 & 0 & 0 & 0 & 0 & 0 \\ 0 & 1 & 0 & 0 & 0 & 0 & 0 \\ 0 & 0 & 1 & 0 & 0 & 0 & 0 \\ 0 & 0 & 0 & 1 & 0 & 0 & 0 \end{pmatrix} \tag{4.17}$$

$$R_t = \begin{pmatrix} \sigma_\phi^2 & 0 & 0 & 0 \\ 0 & \sigma_\lambda^2 & 0 & 0 \\ 0 & 0 & \sigma_{V_E}^2 & 0 \\ 0 & 0 & 0 & \sigma_{V_N}^2 \end{pmatrix} \tag{4.18}$$

$$Z_t = \begin{pmatrix} \phi^{RISS} - \phi^{GPS} \\ \lambda^{RISS} - \lambda^{GPS} \\ V_E^{RISS} - V_E^{GPS} \\ V_N^{RISS} - V_N^{GPS} \end{pmatrix} \tag{4.19}$$

Where:

- σ_ϕ^2, σ_λ^2 is the variance in the latitude and the longitude positions of the GPS measurement, respectively.
- $\sigma_{V_E}^2$, $\sigma_{V_N}^2$ is the variance in the east and the north velocities of the GPS measurement, respectively.
- $\left(\phi^{RISS} - \phi^{GPS}\right)$ is the error between RISS and GPS latitude positions.
- $\left(\lambda^{RISS} - \lambda^{GPS}\right)$ is the error between RISS and GPS longitude positions.
- $\left(V_E^{RISS} - V_E^{GPS}\right)$ is the error between RISS and GPS east velocities.
- $\left(V_N^{RISS} - V_N^{GPS}\right)$ is the error between RISS and GPS north velocities.

The proposed cooperative localization technique is introduced in Subsection 4.4.2 where the above scheme is modified to GPS-free environments.

4.4.2 Proposed Cooperative RISS/RTT using Extended Kalman Filter (EKF)

The above integrated GPS/RISS scheme is updated in both prediction and measurement phases to compensate the unavailability of the GPS signals. EKF is used to predict the error state vector δX to enhance the RISS positions using cooperation between vehicles instead of GPS updates discussed in Subsection 4.4.1. δX implemented in this work is shown in Eq. 4.20 in which δx and δy are used instead of $\delta\phi$ and $\delta\lambda$ since the information from the sensors are directly related to an error in the x and y positions as mentioned earlier. The cooperative information does not provide any updates for velocity measurements (no Doppler shift velocity updates as in GPS), therefore the error in velocities δV_E and δV_N were not considered as in Eq. 4.8. Moreover, δA and δw_z were ignored since the vehicles were moving in straight lines and there was no significant

change in the azimuth angle to be taken into account. Furthermore in typical urban areas, vehicles experience minor fluctuations in the acceleration due to high traffic flow, therefore the component δa_{od} was not considered as well. Nevertheless, modern vehicles are equipped with advanced sensors that are associated with low rate of error deviations over time [51].

$$\delta X_t = \begin{pmatrix} \delta x_t & \delta y_t \end{pmatrix}^T \tag{4.20}$$

Prediction Phase:

The state transition matrix F that models the dynamics in the system states each epoch and the noise distribution matrix G are defined in Eq. 4.21 and 4.22, respectively. The error state vector δX is defined mathematically in Eq. 4.23.

$$F_{t,t-1} = \begin{pmatrix} 1 & 0 \\ 0 & 1 \end{pmatrix} \Delta T \tag{4.21}$$

$$G_{t-1} = \begin{pmatrix} 1 & 0 \\ 0 & 1 \end{pmatrix} \Delta T \tag{4.22}$$

$$\delta X = (x,y)^T - X_{est}^T \tag{4.23}$$

Where $X_{est} = (x_{est}, y_{est})$ is the current estimated position vector for the vehicle to be localized (sender vehicle) after RISS mechanization. While (x,y) refers here to the true unknown position of the sender vehicle.

Measurement Phase:

The measured inter-vehicle distance after compensating both the receiver's processing time and the multipath effect is denoted by $d_m^{(n)}$ which is mathematically equivalent to

$$d_m^{(n)} = \sqrt{(x^{(n)} - x)^2 + (y^{(n)} - y)^2} \tag{4.24}$$

In order to linearize the distance in Eq. 4.24, Taylor series expansion is applied while ignoring the higher order terms. In particular, a Taylor series expansion of a non-linear function $f(x,y)$ at a point (x_i, y_i) is computed in Eq. 4.25. Linearization of the inter-vehicle distance is done

at the current position estimate $X_{est} = (x_{est}, y_{est})$ that replaces $X_i = (x_i, y_i)$ as follows in Eq. 4.26.

$$f(x,y) = f(x_i,y_i) + \frac{\partial f}{\partial x}|_{x_i,y_i}(x-x_i) + \frac{\partial f}{\partial y}|_{x_i,y_i}(y-y_i) \tag{4.25}$$

$$d_m^{(n)} = \sqrt{(x^{(n)}-x_{est})^2 + (y^{(n)}-y_{est})^2} + \frac{(x_{est}-x^{(n)})(x-x_{est}) + (y_{est}-y^{(n)})(y-y_{est})}{\sqrt{(x^{(n)}-x_{est})^2 + (y^{(n)}-y_{est})^2}} \tag{4.26}$$

Recalling the estimated distance computed in Eq. 4.5, it can be written as in Eq. 4.27. The difference between the two distances is computed in Eq. 4.28 where it is written in compact form as shown in Eq. 4.29.

$$d_{est}^{(n)} = \sqrt{(x^{(n)}-x_{est})^2 + (y^{(n)}-y_{est})^2} + e \tag{4.27}$$

$$\delta d^{(n)} = d_m^{(n)} - d_{est}^{(n)} = \frac{(x_{est}-x^{(n)})(x-x_{est}) + (y_{est}-y^{(n)})(y-y_{est})}{\sqrt{(x^{(n)}-x_{est})^2 + (y^{(n)}-y_{est})^2}} - e \tag{4.28}$$

$$\delta d^{(n)} = (1_{est}^{(n)})^T \delta X - e \tag{4.29}$$

Where:

$$(1_{est}^{(n)}) = \frac{[(x_{est}-x^{(n)}), (y_{est}-y^{(n)})]^T}{\sqrt{(x^{(n)}-x_{est})^2 + (y^{(n)}-y_{est})^2}} \tag{4.30}$$

For N neighbors, the design matrix H that relates the error difference between the distances $\delta d^{(n)}$ and the state vector δX is computed in Eq. 4.31, while EKF measurement vector Z shown in Eq. 4.32 represents $\delta d^{(n)}$ from all the neighbors.

$$H_t = \begin{pmatrix} \frac{(x_{est}-x^{(1)})}{\sqrt{(x^{(1)}-x_{est})^2+(y^{(1)}-y_{est})^2}} & \frac{(y_{est}-y^{(1)})}{\sqrt{(x^{(1)}-x_{est})^2+(y^{(1)}-y_{est})^2}} \\ \vdots & \vdots \\ \frac{(x_{est}-x^{(N)})}{\sqrt{(x^{(N)}-x_{est})^2+(y^{(N)}-y_{est})^2}} & \frac{(y_{est}-y^{(N)})}{\sqrt{(x^{(N)}-x_{est})^2+(y^{(N)}-y_{est})^2}} \end{pmatrix} \tag{4.31}$$

$$Z_t = \begin{pmatrix} \delta d^{(1)} \\ \vdots \\ \delta d^{(N)} \end{pmatrix} = \begin{pmatrix} d_m^{(1)} - d_{est}^{(1)} \\ \vdots \\ d_m^{(N)} - d_{est}^{(N)} \end{pmatrix} \tag{4.32}$$

Then for final position update, the estimated error vector is used to correct the latest position of the vehicle to be localized according to Eq. 4.33.

$$\begin{pmatrix} x_t \\ y_t \end{pmatrix} = \begin{pmatrix} \delta x_t^+ \\ \delta y_t^+ \end{pmatrix} + \begin{pmatrix} x_{t-1} \\ y_{t-1} \end{pmatrix} \tag{4.33}$$

Where:

- $\begin{pmatrix} \delta x_t^+ \\ \delta y_t^+ \end{pmatrix}$ is the estimated error state vector and consists of the errors in both x and y positions.
- $\begin{pmatrix} x_{t-1} \\ y_{t-1} \end{pmatrix}$ is the last estimated position vector referred to above as $\begin{pmatrix} x_{est} \\ y_{est} \end{pmatrix}$.

Chapter 5

Performance Evaluation

5.1 Simulation Framework

In this section, the simulation environment is illustrated first, followed by the simulated scenarios and parameters. Figure 5.1 represents the simulation environment that consists of the traffic simulator SUMO and the network simulator ns-3 which will be discussed in Subsections 5.1.1 and 5.1.2.

5.1.1 Traffic Simulator: SUMO

The vehicles' traces are generated using SUMO [52] which is an open source microscopic-level road traffic simulator. SUMO generates the movement patterns of vehicles in a given network while considering practical constraints such as minimum gap between vehicles, maximum velocity in the road and the traffic control conditions (i.e. traffic signs and lights). As such, a 2D location is calculated for each vehicle every one second and then exported in trace files that are readable by the network simulator. In our simulation scenario, the road is divided into two lanes with opposite directions where the length and width of each lane are set to 300 m and 3 m, respectively. The inter-vehicle distance is set to be around 3 m which is adequate for the urban scenario in which the cars are moving with low speed. The total number of vehicles is set to $N = 50$ and divided equally between the two lanes. During the simulation scenario, the vehicles move with constant speed suitable for urban canyon areas. The constant speed is changed in each scenario from 3 to 11 m/s. Figure 5.2 shows the SUMO environment at different time epochs in which the speed of the vehicles is set to be equal to 7 m/s. From Fig. 5.2 at $t = 1$ second, the vehicles enter the road network from one of the two sides and continue moving to the other end. As the

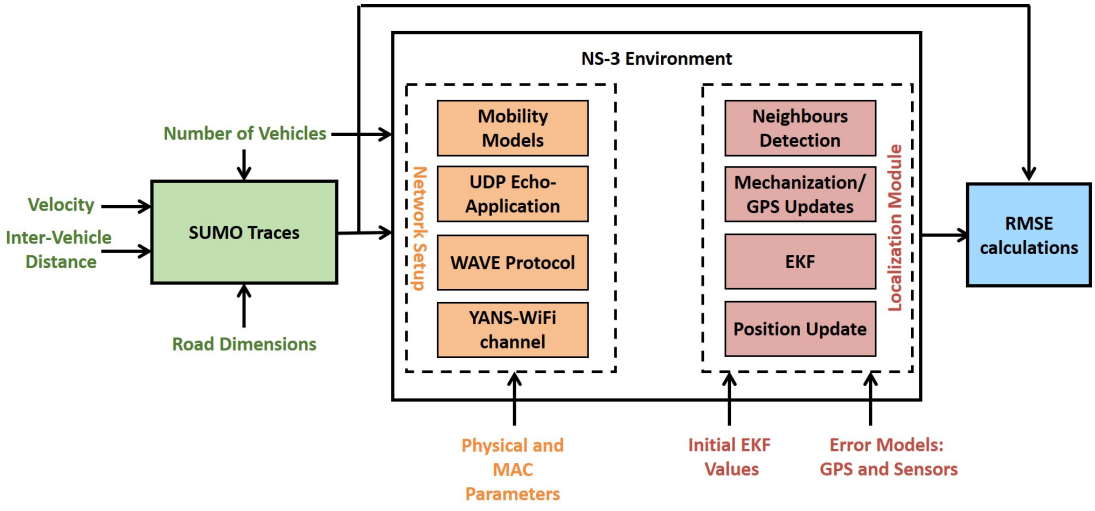

Figure 5.1: Simulation environment

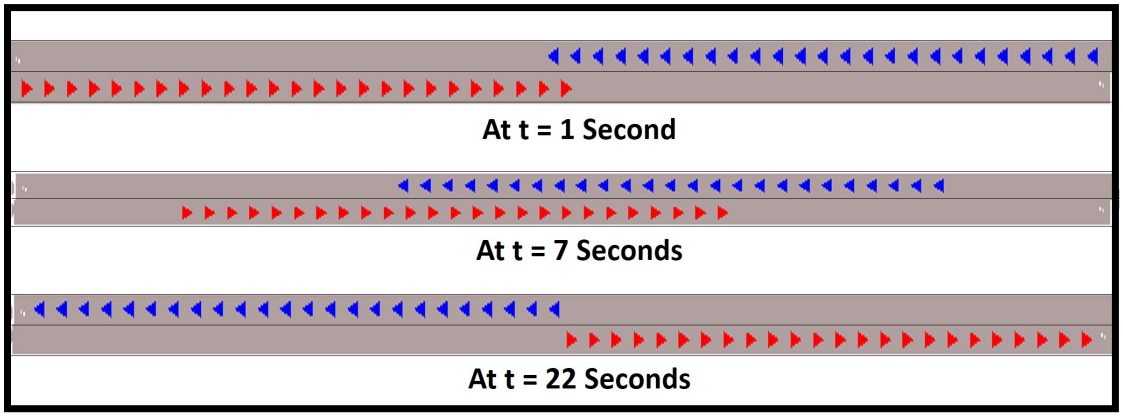

Figure 5.2: SUMO environment at different time epochs for V = 7 m/s

simulation continues, vehicles moving in opposite directions become closer to each other (e.g. at $t = 7$ seconds) before moving apart (e.g. $t = 22$ seconds). For this reason, the duration of the simulation in the implemented scenarios depends on the speed assigned to the vehicles to guarantee that all the vehicles are moving within the road boundaries.

5.1.2 Network Simulation: ns-3

We simulate the proposed cooperative scheme using a VANETs standard compliant network simulator ns-3 [1]for practical evaluation. ns-3 is an open source event-driven communication

[1] **http://www.nsnam.org.**

network simulator which is currently supporting VANETs simulations through its WAVE module. In particular, each vehicle is represented as a node which basically implements three communication layers: application, stack protocol and the network device . In the simulation, each vehicle implements two applications: UDP echo client and UDP echo server. The first application is used to request location messages from the neighboring vehicles while the latter allows the vehicle to receive the LRM from the neighboring vehicles and respond to them according to our scheme flow chart in Fig. 4.1. The stack protocol layer simulates the node's (i.e. vehicle's) network layer which is mainly responsible to assign its ID and address. Finally, the network device layer implements the MAC and physical layer aspects of the vehicle. In essence, we adopt the WAVE module for the MAC and YansWifiPhy module, normal WiFi, for the physical layer which are typically used in VANETs. The vehicles are allowed to communicate through wireless channel implemented by the YansWiFiChannel module which simulates the wireless path loss, propagation and transmission delays experienced by the signal. Moreover, each node has a mobility model that follows the trajectory files generated by SUMO. The cooperative localization technique is then implemented in the ns-3 after the aforementioned network setup phase. In particular, four main functions are added: neighbor detection, mechanization, EKF and position update. The first function is triggered by the transmitted packet by the UDP echo client application of the vehicle to be localized that continues to store the received information from the UDP echo server application of the neighbors. Such information is then forwarded to the mechanization function and then to the EKF for calculating the position errors. Finally, this error is used to update the current known location of the vehicle (not the mobility model) and will be used by its UDP echo server application for localization of other vehicles.

5.1.3 Simulation Parameters

For simulation parameters, we adopt typical values from the standards and existing practical studies. Location update interval is set by the packet arrival rate of the UDP echo application which is set to 1 second for efficient spectrum utilization and avoiding network congestion. The initial parameters of the EKF are extensively tuned to minimize the RMSE and reflect the variance in the measured distances as well as the process noise. However, the simulations will consider mul-

EKF Parameters	Value
F_{t-1}	$\begin{pmatrix} 1 & 0 \\ 0 & 1 \end{pmatrix}$
G_{t-1}	$\begin{pmatrix} 1 & 0 \\ 0 & 1 \end{pmatrix}$
W_{t-1}	$\begin{pmatrix} 0 \\ 0 \end{pmatrix}$
R_t	$I_{N\times N}$
Ideal Initial Position: Q_{t-1}	$\begin{pmatrix} 0.3 & 0 \\ 0 & 0.001 \end{pmatrix}$
Ideal Initial Position: P_0^+	$\begin{pmatrix} 0.01 & 0 \\ 0 & 0.01 \end{pmatrix}$
Erroneous Initial Position: Q_{t-1}	$\begin{pmatrix} 0.3 & 0 \\ 0 & 0.5 \end{pmatrix}$
Erroneous Initial Position: P_0^+	$\begin{pmatrix} 1 & 0 \\ 0 & 1 \end{pmatrix}$

Table 5.1: Kalman filter simulation parameters

tiple scenarios with different error sources for extensive evaluation and thus the EKF parameters are changed as illustrated in Table 5.1.

Simulating Sensor Errors:

The ideal measurements of the gyroscope and odometer are imported from SUMO. For practical simulation of the mechanization process, random Gaussian errors are added to both the gyroscope and odometer values as mentioned in Section 4.2. The odometer's error follows a Gaussian distribution with 0 mean and standard deviation equal to 10% from the speed of the vehicle as simulated in [53] and [6]. Thus, the increase in the odometer error is proportional to the distance traveled by the vehicle [54]. For the simulated gyroscope, the error introduced is ARW, which also follows Gaussian distribution with mean 0 and standard deviation chosen to be equal to $2^\circ/\sqrt{hr}$ for a specific model according to [49].

Simulating GPS Errors:

In some scenarios, we assume erroneous GPS measurements either in the initial positions or the frequent position updates when the vehicles have an open sky access. Such measurements are assumed to yield a maximum position error of z meters. This is typically modeled by adding a Gaussian distributed random variable e_P with 0 mean and variance σ_p^2 whose value depends on the maximum error z and can be calculated as follows:

Error Models	Value
Odometer Error	$\approx N\left(0,(0.1\times speed)^2\right)$
Gyroscope ARW Error	$\approx N(0,4)$
For $z_{GPS}=5$ m	$\approx N(0,1.39)$
For $z_{GPS}=3$ m	$\approx N(0,0.5)$
For $z_{GPS}=2$ m	$\approx N(0,0.22)$

Table 5.2: Error modeling

Assume that the CDF of the GPS error should have most of the points below z (i.e. 99.7%). Thus

$$\mu + 3\sigma_p = z \tag{5.1}$$

For $\mu = 0$:

$$\sigma_p = \frac{z}{3} \tag{5.2}$$

To calculate the error variance in x and y positions:

$$\sigma_p^2 = \left(\sqrt{\sigma_x^2 + \sigma_y^2}\right) \tag{5.3}$$

Assume $\sigma_x = \sigma_y = \sigma_{xy}$

$$\sigma_p^2 = \left(\sqrt{2\times\sigma_{xy}^2}\right)^2 = \left(\frac{z}{3}\right)^2 \tag{5.4}$$

$$\therefore \sigma_{xy}^2 = \left(\frac{z}{3}\right)^2 \times \frac{1}{2} \tag{5.5}$$

Where σ_{xy}^2 is the variance in each of x and y directions.

The different values of σ_{xy}^2 with the corresponding maximum error z and the error modeling of the sensors are shown in Table 5.2. All other physical layer and application parameters are

ns-3 Parameters	Value
Propagation Loss Model	$Log\,distance$
Propagation Delay Model	$Constant\,speed$
Minimum Received Power	$-105\,dBm$
Different Sensitivity Levels	$-85\,dBm, -75\,dBm, -65\,dBm$

Table 5.3: ns-3 Simulation parameters

summarized in Table 5.3.

5.1.4 Overview of Simulated Scenarios

To evaluate the performance and the localization accuracy of the introduced cooperative scheme, different scenarios of vehicle movements and error models are considered. The objective of this scheme is to have a good localization accuracy in urban areas compared to the typical localization techniques used. In this proposed technique, EKF uses the updated positions of the vehicles using RISS mechanization with the inter-vehicle distances obtained using RTT for final position estimate. This technique is evaluated compared to the RISS technique in urban canyons with total GPS blockage assuming ideal initial position and then extended to the erroneous case. Additionally, the performance of the scheme is studied in case of having GPS updates with distinct variances and also evaluated by comparing various percentage of vehicles with GPS updates. Furthermore, diverse densities of neighboring vehicles are also taken into consideration. Then this cooperative technique is compared to widely used non-cooperative and cooperative techniques.

5.2 Simulation Results

5.2.1 Evaluation Metrics

The evaluation metrics used in the simulation are the average Root Mean Square Error $R\bar{M}SE_t$ and the maximum root mean square error $R\hat{M}SE_t$ between the true position (obtained from SUMO) and the estimated position from the localization scheme calculated as follows:

$$R\bar{M}SE_t = \frac{\sum_{i=1}^{N} \sqrt{(x_{i,t} - \hat{x}_{i,t})^2 + (y_{i,t} - \hat{y}_{i,t})^2}}{N \times S}, \forall t \in T \tag{5.6}$$

$$\hat{RMSE}_t = \max_{\forall i \in \{1,..N\}} \frac{\sqrt{(x_{i,t} - \hat{x}_{i,t})^2 + (y_{i,t} - \hat{y}_{i,t})^2}}{S}, \forall t \in T \tag{5.7}$$

Where:

- $x_{i,t}$, $y_{i,t}$ is the true position obtained from SUMO.
- $\hat{x_{i,t}}$, $\hat{y_{i,t}}$ is the estimated position using the localization scheme.
- S is the number of simulations.
- N is the total number of vehicles.
- i is the index of each vehicle.
- t is the time epoch.
- T is the total duration of one simulation.

In particular for a cluster of N vehicles over a period of time T, the average RMSE at certain time instant $\bar{RMSE}_t$ is calculated by taking the average of the RMSE of the vehicles' positions as in Eq. 5.6. This metric is used as it gives an average overview of the performance of the vehicles in different scenarios (e.g. vehicle in the middle of the road surrounded by many neighbors or vehicle at the edge with lower number of neighbors).

The maximum RMSE at a given time $\hat{RMSE}_t$ represents the worst case scenario of a vehicle which might suffer from large sensor errors, a small number of surrounding neighbors or low accuracy in the neighbors' positions and is calculated as shown in Eq. 5.7. All the simulated scenarios consider errors in inertial sensors and/or positions updates, and thus all results are averaged over S runs for statistical validation. We computed the confidence intervals for a 95% confidence level. The confidence intervals were found to be small for all simulations, and hence were not explicitly depicted in the figures. All the evaluation metrics parameters used in the simulations are given in Table 5.4. Our introduced Cooperative Localization (CL) scheme is evaluated in the coming sections and it is written in short as CL KF-RISS.

Evaluation Metric Parameters	Value
N	50
S	50
For $V = 3$ m/s: T_{max}	50 seconds
For $V = 5$ m/s: T_{max}	30 seconds
For $V = 11$ m/s: T_{max}	10 seconds

Table 5.4: Evaluation metric parameters

5.2.2 Comparison of the Proposed Cooperative Scheme with the Non Cooperative RISS

As mentioned earlier, one of the considered scenarios is that all the vehicles have initial positions obtained either from GPS or any other localization system and then, these vehicles travel in urban canyons or tunnels with total absence of GPS. Thus to evaluate the performance of the proposed cooperative localization scheme, it is compared with respect to the 2D RISS since the latter is the typically used localization technique in urban canyons and tunnels with GPS blockage. The effect of the accuracy of the initial position on the schemes' performance is then studied.

5.2.2.1 Ideal Initial Position

In this evaluation scenario, the average and the maximum RMSE of the proposed cooperative scheme is compared with respect to those of the 2D RISS technique for different velocities assuming perfect initial positions as shown in Fig. 5.3 and 5.4 respectively. In both figures, the non-cooperative RISS suffers from rapid diversions from the true positions (RMSE increased dramatically) over time compared to the cooperative scheme. The enhancement in our proposed cooperative scheme is attributed to the frequent updates from the ranging technique RTT and the RISS-based more accurate neighbors' positions. In particular, the EKF was able to use the RTT measurements in order to correct the RISS-based predicted position's error and thus limits its accumulation over time. Therefore, for a duration of 10 seconds, the maximum RMSE of the proposed scheme has all the values smaller than 1 m compared to the RMSE of the RISS which has values up to 8 m. Such enhancement is also attained at higher velocities where the performance of RISS is highly degraded due to the increased error variance in the odometer according to the model used [53].

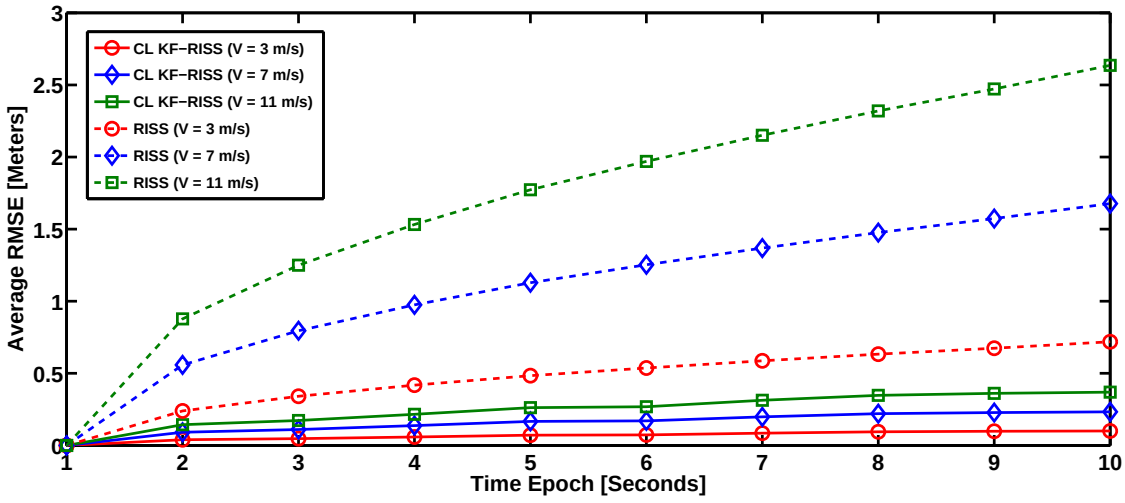

Figure 5.3: Average RMSE comparison between the proposed scheme and 2D RISS (Ideal initial positions)

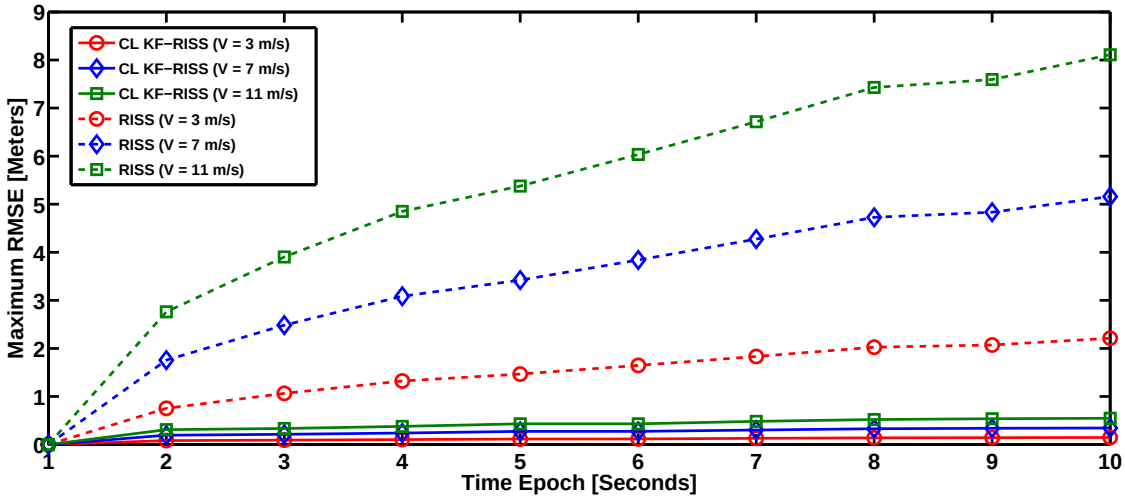

Figure 5.4: Maximum RMSE comparison between the proposed Scheme and 2D RISS (Ideal initial positions)

5.2.2.2 Erroneous Initial Position

Our evaluation scenario is extended by introducing an error in the initial position that follows a Gaussian distribution with variance equal to 1.39 as mentioned in Table 5.2. This variance is suitable for capping the GPS position error below 5 m. The EKF parameters require tuning based on the newly added source of errors (inaccurate initial positions). In particular, the initial value of the P matrix in Table 5.1 was increased to reflect the uncertainty in the erroneous initial position. Practically, this value can be also obtained from the standalone positioning system used in obtain-

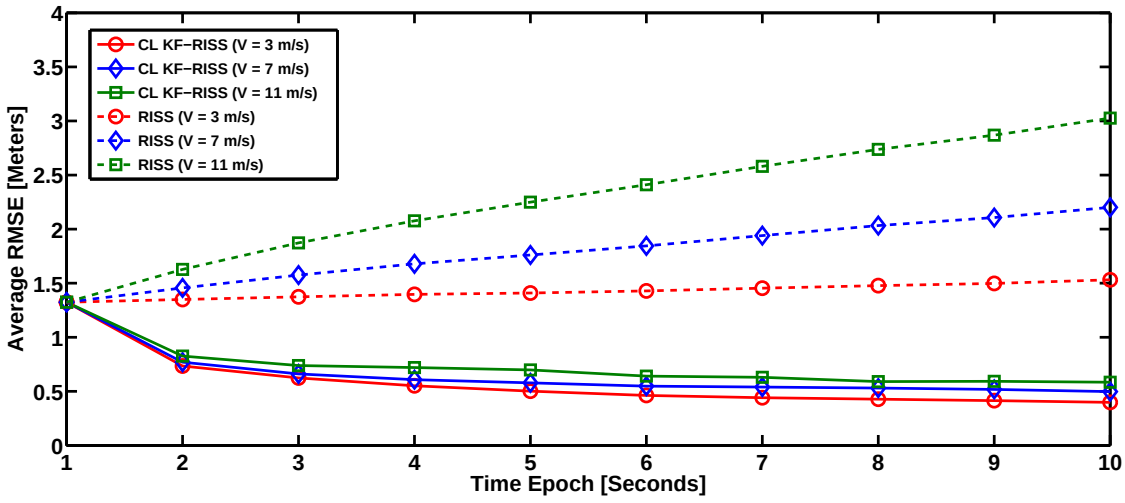

Figure 5.5: Maximum RMSE comparison between the proposed scheme and 2D RISS (Erroneous initial positions)

ing the initial position of each vehicle. Similarly, the Q matrix entry that corresponds to the error in the y position is increased to compensate the error in the initial position compared to the ideal initial position scenario discussed previously with no error in the y position since the vehicle was moving only in a straight line in the x direction. Comparing the two schemes as shown in Fig. 5.5, the proposed cooperative scheme continues to outperform the 2D RISS over the trajectory. From the figure, the cooperative scheme was able to correct the inaccurate initial vehicles' positions using the ranging technique and the enhanced neighbors' positions. Thus, vehicles with low location error can improve the position of other vehicles with higher error using the measured distance d_m. Conversely, this enhancement is not achievable in the RISS since each vehicle continues to deviate over time from the true position as a result of error accumulation.

5.2.3 Proposed Cooperative Scheme Evaluation: Effect of Different Neighbors' Densities and Sensitivity Levels

In the above scenarios, the sensitivity level (i.e. minimum received power to decode the received signal) of all the vehicles was fixed at -105 dBm. This small value resulted in large communication range that allows cooperation between all the considered vehicles. In order to evaluate the effect of the neighbors' density on the performance of our localization scheme, the above sensitivity is increased to $-85, -75$ and then to -65 dBm. Thus, fewer neighbors will receive and respond to the LRM. Practically, these effects can be achieved by decreasing the transmitted power

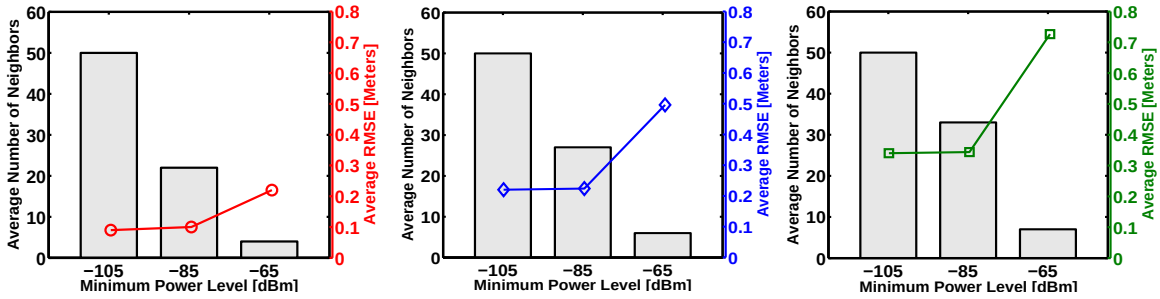

(a) At velocity = 3 m/s (b) At velocity = 7 m/s (c) At velocity = 11 m/s

Figure 5.6: Effect of neighbor's densities on the average RMSE of the proposed cooperative scheme

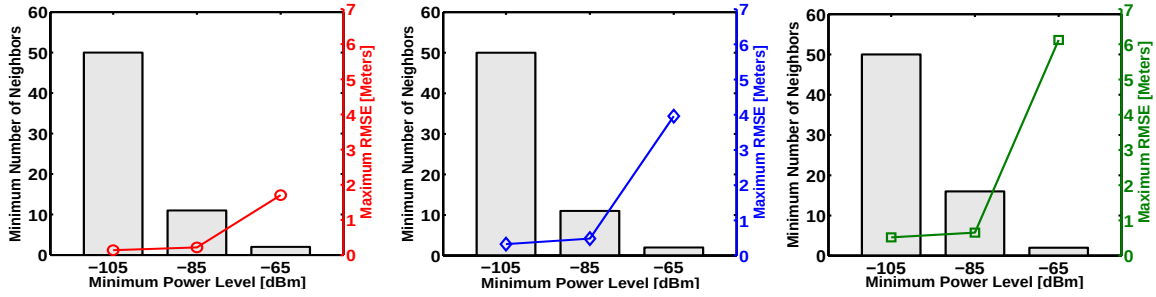

(a) At velocity = 3 m/s (b) At velocity = 7 m/s (c) At velocity = 11 m/s

Figure 5.7: Effect of neighbor's densities on the maximum RMSE of the proposed cooperative scheme

which is desirable for many reasons such as minimizing interference, increasing bandwidth efficiency and decreasing the energy consumption in the network. Figures 5.6 and 5.7 show the effect of the different sensitivity levels that reflects the number of neighbors used in the localization on the RMSE for the three different velocities with the presence of error in the inertial sensors assuming ideal initial positions. We have chosen an arbitrary time which is the middle of the simulation time so that the vehicles moving in opposite directions are within the coverage range of each other. At $t = 6$ seconds, the average RMSE is compared to the average number of neighbors for the different velocities shown in Fig. 5.6 (a), (b) and (c). In Fig. 5.7, the minimum number of neighbors is compared to the corresponding maximum value of RMSE. In both cases, RMSE increases when the total number of neighbors used in localization decreases and/or the velocity of the vehicles increases. In Fig. 5.7 (c), the minimum number of neighbors becomes two at power level equal to -65 dBm which is the minimum number needed by the EKF to obtain a solution. Figures 5.8

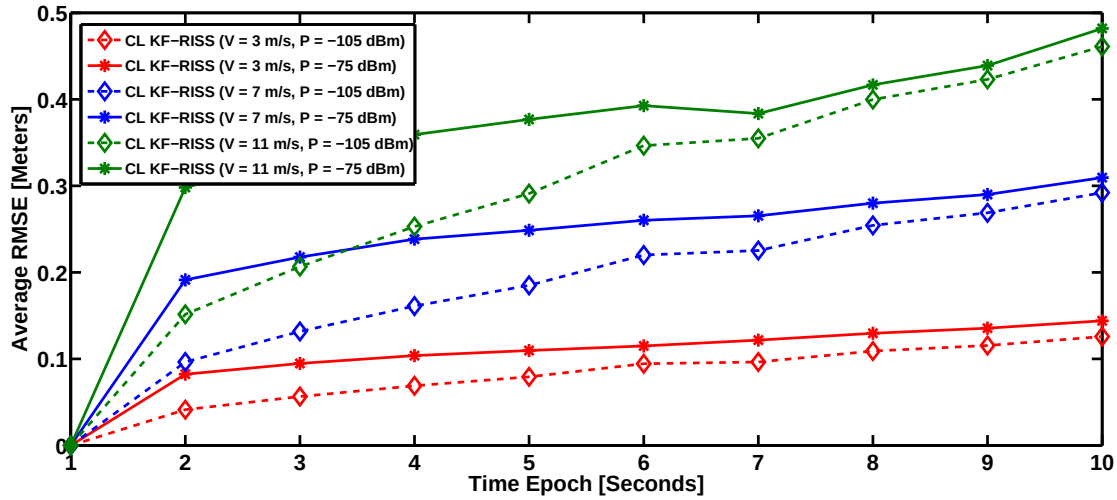

Figure 5.8: Effect of the different sensitivity levels on the average RMSE of the proposed cooperative scheme

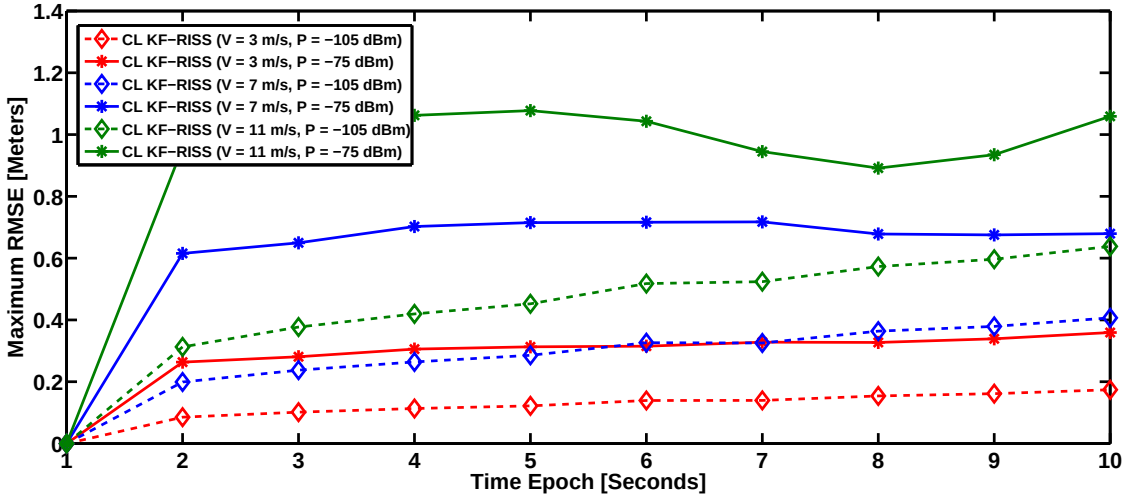

Figure 5.9: Effect of the different sensitivity levels on the maximum RMSE of the proposed cooperative scheme

and 5.9 show the effect of two different power levels on the localization accuracy over the time. As the sensitivity level and/or the velocity of the vehicles increases, the average RMSE is worse, as is the maximum RMSE. In these two latter figures, the power level is only increased to -75 *dBm* to guarantee that the minimum number of neighbors surrounding each vehicle is greater than 2. These results demonstrate the importance of increasing the communication range in the case of fast moving vehicles in order to compensate the growing error variance of the RISS adopted in the cooperative scheme.

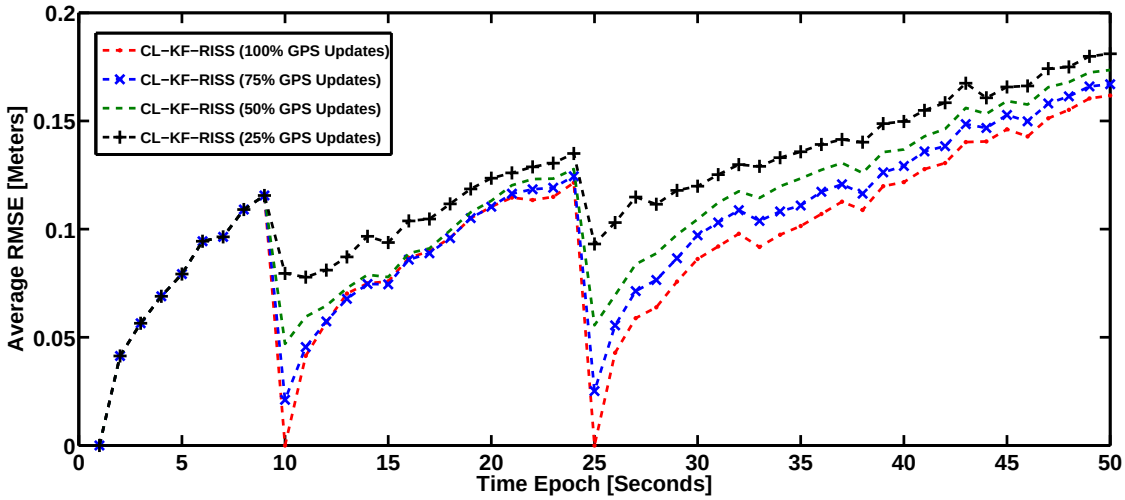

Figure 5.10: Effect of different percentages of vehicles with ideal GPS updates on the average RMSE

5.2.4 Proposed Cooperative Scheme Evaluation: Effect of GPS Updates

Another simulated scenario is implemented where it is assumed that at certain time epochs, either all or portion of the vehicles have an open sky access and thus receive GPS position updates. To evaluate the performance of the proposed scheme, the following scenarios are considered.

5.2.4.1 Ideal GPS Updates

At $t = 10$ and $t = 25$ seconds, it was assumed that all the vehicles can receive clear and ideal signals from the GPS satellites and thus these vehicles can have an updated position with approximately no error. After that, these vehicles experience GPS blockage again and the cooperative scheme is used. Different percentages of vehicles with GPS updates are evaluated compared to the ideal scenario in which all the vehicles receive GPS updates to test the effect on the average and the maximum RMSE as shown in Fig. 5.10 and 5.11. 25%, 50% and 75% of vehicles with ideal GPS updates are implemented and compared to each other and with respect to the aforementioned ideal scenario. In addition to enhancing the RMSE of the vehicles with GPS updates, the cooperative scheme was able to broadcast these enhancements to the neighboring vehicles still experiencing GPS blockage. Such cooperation results in enhancing the neighbors' positions as illustrated in Fig.

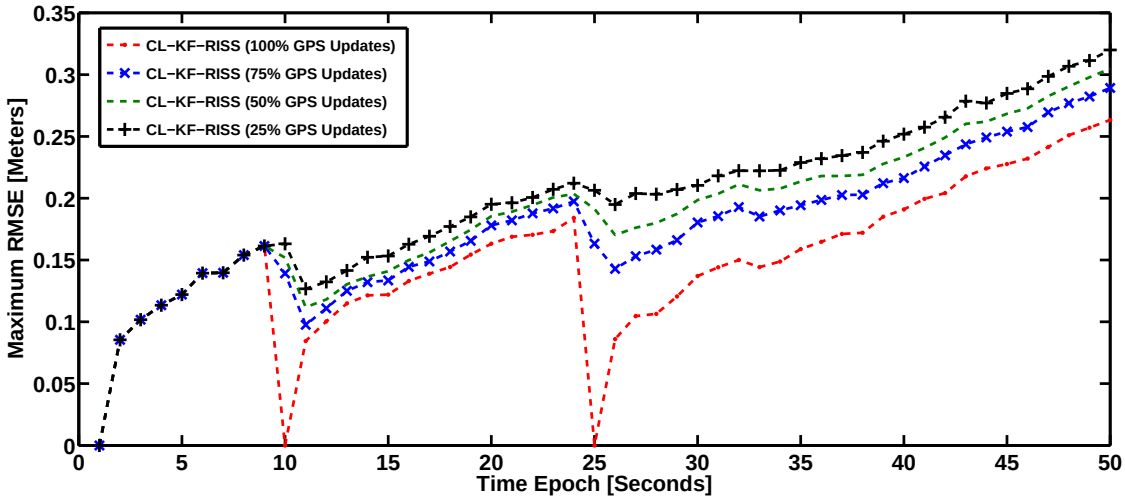

Figure 5.11: Effect of different percentages of vehicles with ideal GPS updates on the average RMSE

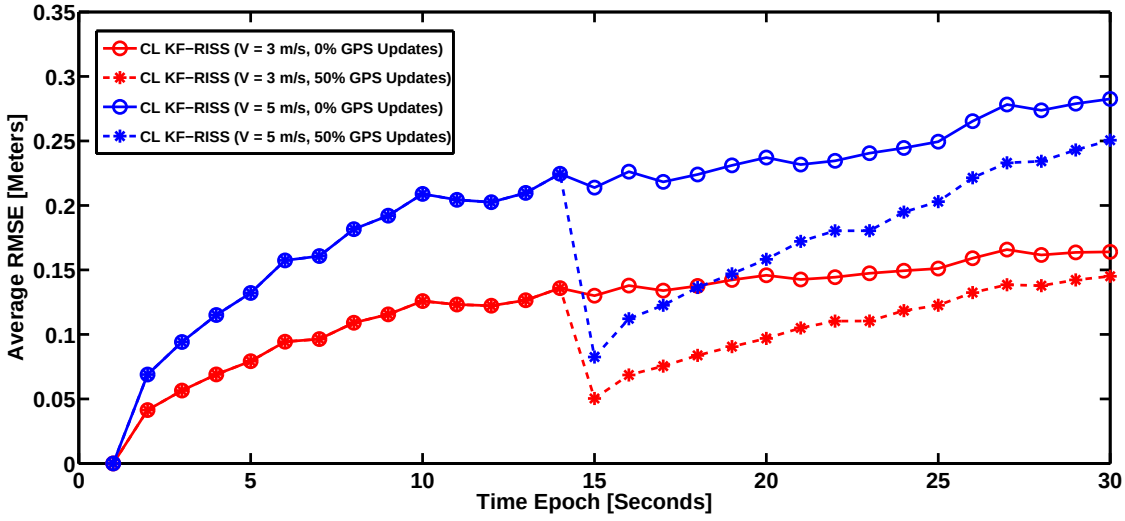

Figure 5.12: Average RMSE of different percentage of ideal GPS updates on different velocities

5.10 where the percentage of RMSE enhancement is higher than the percentage of GPS updates.

5.2.4.2 Ideal GPS Updates at Different Velocities

The above mentioned cooperative gain during GPS updates is emphasized when higher velocities are considered as shown in Fig. 5.12 and Fig. 5.13 . While higher velocities suffer from rapid increase in RMSE, the cooperative scheme was able to limit such deterioration with partial GPS updates to the network.

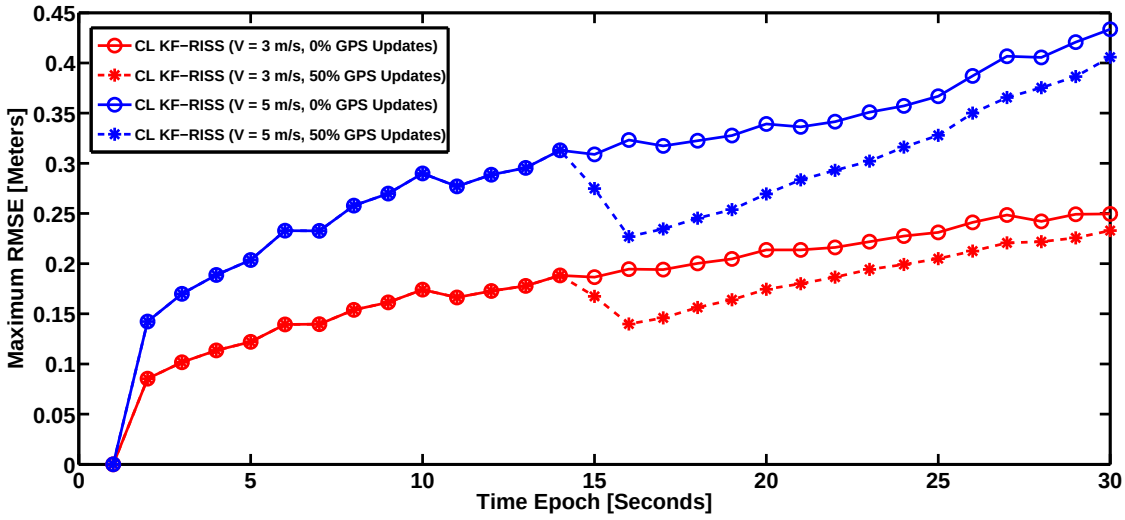

Figure 5.13: Maximum RMSE of different percentage of ideal GPS updates on different velocities

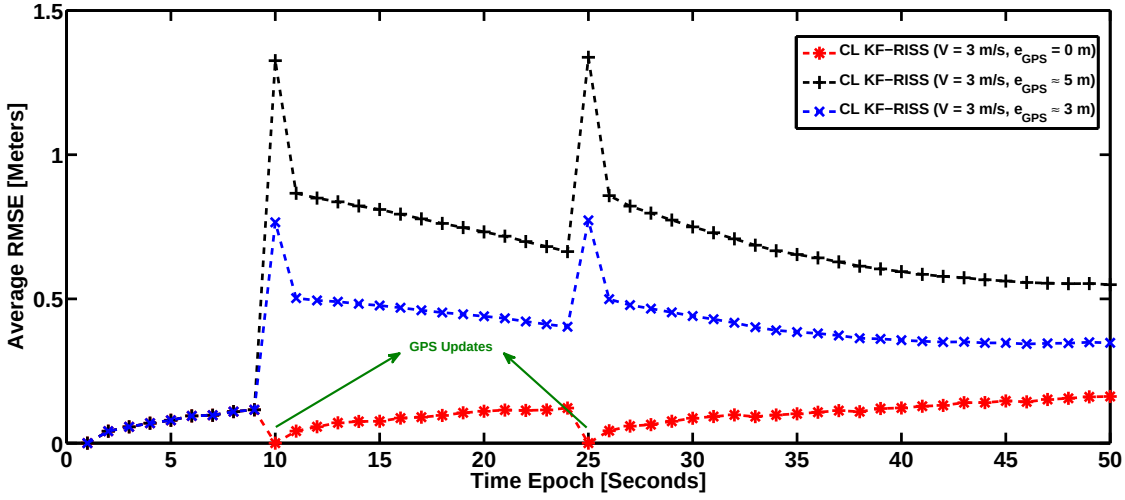

Figure 5.14: Effect of erroneous GPS updates on the average RMSE

5.2.4.3 Erroneous GPS Updates with Different Variances

Practically, any position obtained using GPS or any other localization technique is subjected to error due to the environment as previously discussed in Chapter 2. For this reason, at the selected time slots ($t = 10$ and $t = 25$), we assume that all the vehicles have erroneous GPS updates. Different variances of errors of 1.39 and 0.5 are implemented that reflect a max error of 5 m and 3 m and compared to GPS updates with zero error. Figure 5.14 and Fig. 5.15 show the average RMSE and the maximum RMSE over 50 seconds for vehicles moving with velocity equal to 3 m/s. From these two figures, the erroneous GPS updates affects the performance of the coop-

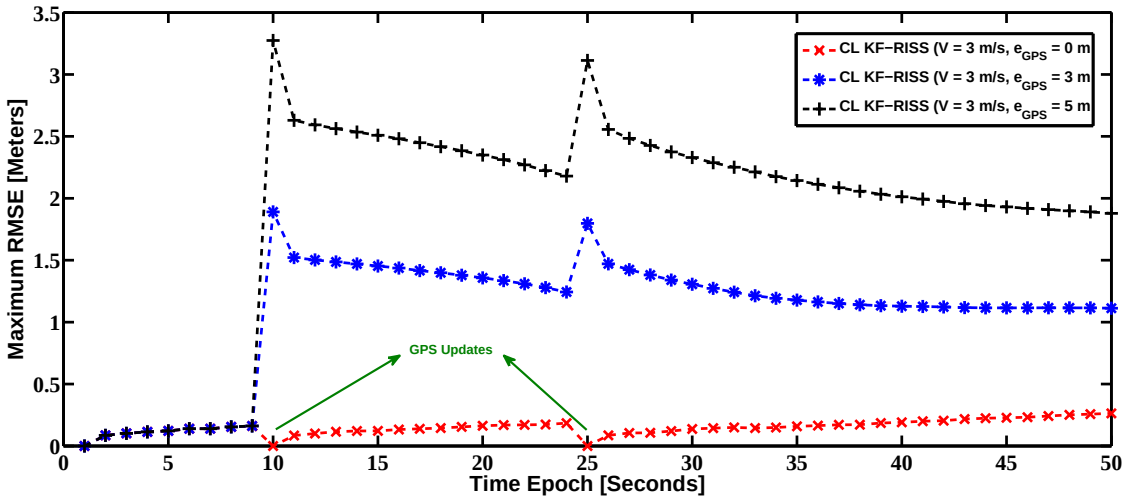

Figure 5.15: Effect of the erroneous GPS updates on the maximum RMSE

erative scheme and make the average and the maximum RMSE worse. This is because the error introduced in the GPS position is larger compared to the errors in the motion sensors (odometer and gyroscope) and also because the proposed scheme enhances the motion sensors' errors using cooperation . Therefore, GPS updates will only enhance the proposed scheme performance whenever the error variance of the GPS is less than the error variance of the RISS.

5.2.5 Proposed Cooperative Scheme Evaluation: Comparison with Other Existing Localization Systems

The average of the RMSE and the maximum of the RMSE of the proposed cooperative scheme is compared with three other existing localization systems. The first is the RISS technique discussed in 2.1.2.2, the second is another non-cooperative scheme written in short as Non-CL GPS which is based on only having GPS positions with variances 0.22 and 1.39 that correspond to a maximum error of 2 m and 5 m. The third technique is a cooperative scheme to enhance GPS positions widely used in the literature [41] written here in short as CL KF-GPS. The CL KF-GPS scheme is updated in this work to have a similar structure and thus complexity to our introduced cooperative scheme. In essence, CL KF-GPS assumes that all the vehicles have open sky access, and thus the sender's and neighbors' positions are updated using GPS measurements instead of the RISS with variance 0.22 corresponding to a maximum error of 2 m.

In all the scenarios, the velocity of the vehicles is set to 11 m/s and the duration of the

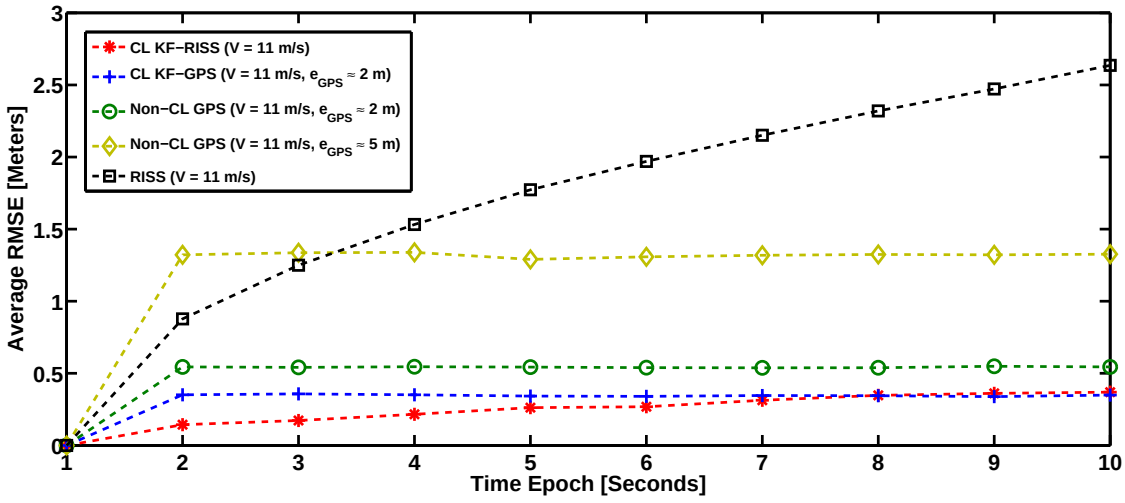

Figure 5.16: Average RMSE comparison between the proposed cooperative scheme and the other existing localization systems

simulation to 10 seconds to guarantee that all the vehicles are in the communication range of each other and the only sources of the error are the sensors or GPS measurements irrespective of the density of neighboring vehicles. We recall, that the proposed cooperative scheme localizes all vehicles using the RISS technique and then enhances these positions by cooperation with RTT-based range estimation. The sources of errors in this scheme are because of the errors associated with the motion sensors (odometer and gyroscope) and the mechanization process.

Generally, the non-cooperative RISS scheme outperforms the non-cooperative GPS only for a very short term (i.e. 3 seconds in Fig. 5.16) while this is not the case for smaller GPS error variances that dominate for the whole duration. In addition, such duration becomes smaller with regards to the maximum RMSE as shown in Fig. 5.17 . All the above is attributed to the typical accumulation of the large errors associated with the odometer in the high velocities.

The introduced cooperative scheme was able to extend the above short duration beyond 10 seconds while considering multiple low noise GPS experienced by the cooperative GPS scheme.

In conclusion, the cooperative scheme was able to considerably stabilize the performance of the RISS which was found previously to deviate with time in the non-cooperative form. Thus, dependency on cooperative RISS for longer time duration can provide acceptable localization accuracy.

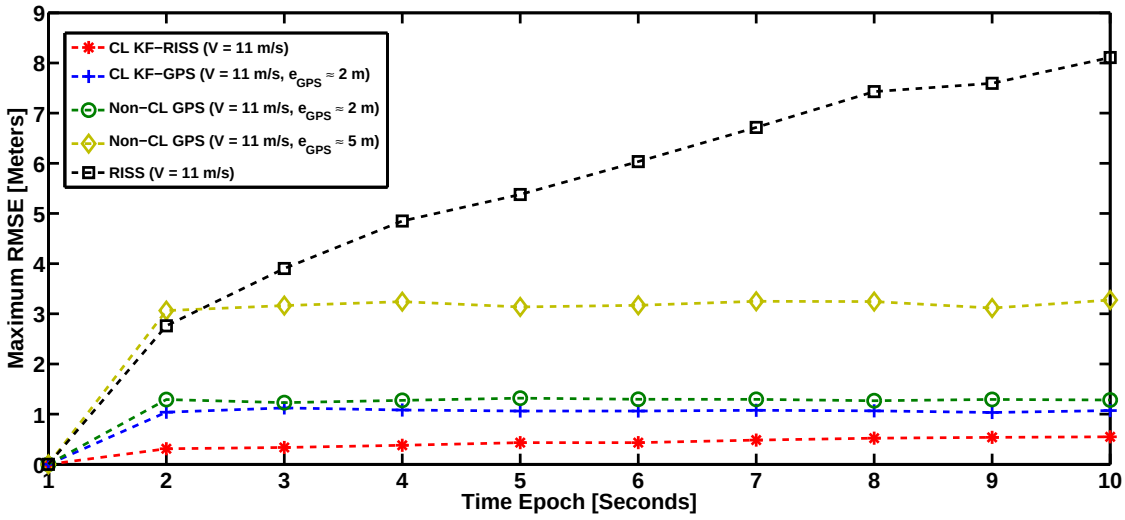

Figure 5.17: Maximum RMSE comparison between the proposed cooperative scheme and the other existing localization systems

5.3 Cooperative Scheme Complexity

In order to assess the practicality of the proposed cooperative scheme, we compute its complexity. The first main block, LRM, has an $O(N^2)$ complexity as the vehicle will check the sender's ID in all the received messages, where N is the number of all the vehicles. This scenario corresponds to the worst case in which all the vehicles are requesting and responding to the LRM for all the vehicles in the system. As such, each vehicle has to filter its own LRM responses and then decodes neighbors' information for the next stages.

The second and the third stages have lower complexity $O(N)$. The mechanization is a linear operation that is done for all the responded $N-1$ neighbors and for the vehicle to be localized. Similarly, the calculation of both distances is done for all the $N-1$ neighbors using Eq. 4.5 and 4.7. The final stage implements the EKF that comprises matrix operations such as inverse and multiplication. Accordingly, the complexity will be $O(N^3)$ for both operations.

Chapter 6

Conclusion and Future Work

6.1 Summary and Conclusion

Our proposed cooperative localization technique is introduced to provide vehicles with high position accuracy in GPS-free environments. The scheme integrates the neighbors' updated positions using RISS mechanization with the measured inter-vehicle distances using RTT through EKF. Error models were introduced to the motion sensors (odometer and gyroscope) and the position updates for practical purposes. The scheme succeeded to limit the errors of the sensors, the neighboring vehicles positions and the mechanization process. Traffic traces were exported from SUMO and the scheme was implemented and tested on ns-3. Different scenarios were simulated to test the robustness of the proposed scheme for different velocities, vehicle densities, GPS availability and error models.

First, the effect of different velocities as well as the accuracy of the initial position on the performance of the proposed cooperative scheme compared to the non-cooperative RISS technique is evaluated. The RMSE is large for higher velocities because the error introduced to the odometer is a percentage of the vehicle's speed. For all values of velocity, the proposed cooperative scheme outperforms the RISS over the whole time horizon due to the ability of the ranging technique to limit the error accumulation of the mechanization process. Second the sensitivity levels for all the vehicles are increased to study the effect of the neighbors' densities on the RMSE. The results demonstrated the importance of extending the communication range of fast moving vehicles in order to cooperate with as many neighbors as possible and thus limit and compensate the large error of the mechanization.

Due to the fact that vehicles can acquire GPS positions at certain time epochs, the perfor-

mance of the cooperative scheme is only enhanced when the GPS error variance is less than the errors associated in the RISS within the proposed technique. Moreover, vehicles with GPS updated positions were able to share such enhancement among the network. Thus, decreases the RMSE of the surrounding neighbors with blocked GPS compared to the scenario of non-GPS updates in the network.

Moreover, the proposed cooperative scheme, utilizing RISS under complete GPS outage, was compared to both the non-cooperative RISS and GPS as well as cooperative GPS-based scheme with different accuracies. Results demonstrated the ability of the proposed cooperative scheme to extend the reliability of RISS for a longer duration compared to the non-cooperative case. In particular, the cooperative scheme can outperform the low noise GPS cooperative scheme over a longer time duration compared to the non-cooperative forms of both techniques.

6.2 Future Work

We recommend the following research points for the future related work:

1) Introduce weighting functions to evaluate and select the neighbors with high accuracy and certainty in their positions, then update the EKF model accordingly. Neighbors with recent high accurate GPS position updates will have more weights compared to the others relying on RISS or cooperative scheme for a long time duration. These weights have to be then incorporated in the noise covariance matrix in the EKF.

2) Evaluate the introduced scheme in the light of location-based services simulated within the same framework. In particular, ns-3 can simulate location-based services and provide end to end performance evaluation under a given location accuracy. Thus, incorporating the introduced cooperative scheme in such scenarios will provide more insights on its reliability and adequacy for the location-based applications.

3) Extend the performance evaluation to a) consider more complicated SUMO traces with different velocities and directions of movement, b) incorporate real range, sensors and GPS measurements for practical assessment.

Bibliography

[1] R. Atawia, H. Abou-zeid, H. S. Hassanein, and A. Noureldin, "Robust resource allocation for predictive video streaming under channel uncertainty," in *Proc. IEEE GLOBECOM*, 2014, pp. 4683–4688.

[2] A. Boukerche, H. A. Oliveira, E. F. Nakamura, and A. A. Loureiro, "Vehicular ad hoc networks: A new challenge for localization-based systems," *Elsevier Computer Commun.*, vol. 31, no. 12, pp. 2838–2849, 2008.

[3] T. L. Willke, P. Tientrakool, and N. F. Maxemchuk, "A survey of inter-vehicle communication protocols and their applications," *IEEE Commun. Surveys Tuts.*, vol. 11, no. 2, pp. 3–20, 2009.

[4] F. C. Commission, "Amendment of the commission rules regarding dedicated short-range communication service in the 5.850-5.925 ghz band," fcc 02-302. Technical report, FCC, Tech. Rep., 2002.

[5] N. Alam and A. G. Dempster, "Cooperative positioning for vehicular networks: facts and future," *IEEE Trans. Intell. Transp. Syst.*, vol. 14, no. 4, pp. 1708–1717, 2013.

[6] E.-K. Lee, S. Y. Oh, and M. Gerla, "Rfid assisted vehicle positioning in vanets," *Elsevier Perv. Mobile Comput.*, vol. 8, no. 2, pp. 167–179, 2012.

[7] C.-H. Ou, "A roadside unit-based localization scheme for vehicular ad hoc networks," *Int. J. Commun. Syst.*, vol. 27, no. 1, pp. 135–150, 2014.

[8] A. Noureldin, T. B. Karmat, and J. Georgy, "Fundamentals of inertial navigation, satellite-based positioning and their integration," Springer, 2013.

[9] A. Bahillo, J. Prieto, S. Mazuelas, R. M. Lorenzo, J. Blas, and P. Fernández, "IEEE 802.11 distance estimation based on rts/cts two-frame exchange mechanism," in *Proc. IEEE VTC*, 2009, pp. 1–5.

[10] M. Marchenko, A. Ramirez, and C. Schwingenschlögl, "Method for calibrating a propagation-time-based localization system," Jul. 23 2013, US Patent 8,494,556.

[11] H. Kloeden, D. Schwarz, E. M. Biebl, and R. H. Rasshofer, "Vehicle localization using cooperative rf-based landmarks," in *Proc. IEEE IV Symp.*, 2011, pp. 387–392.

[12] M. Elazab, A. Noureldin, and H. S. Hassanein, "Integrated cooperative localization for connected vehicles in urban canyons," in *Proc. IEEE GLOBECOM*, 2015, to appear.

[13] D. E. Manolakis, "Efficient solution and performance analysis of 3-d position estimation by trilateration," *IEEE Trans. Aerosp. Electron. Syst.*, vol. 32, no. 4, pp. 1239–1248, 1996.

[14] H. Qi and J. B. Moore, "Direct kalman filtering approach for gps/ins integration," *IEEE Trans. Aerosp. Electron. Syst.*, vol. 38, no. 2, pp. 687–693, 2002.

[15] S. Rezaei and R. Sengupta, "Kalman filter-based integration of dgps and vehicle sensors for localization," *IEEE Trans. Control Syst. Technol*, vol. 15, no. 6, pp. 1080–1088, 2007.

[16] N. El-Sheimy, K.-W. Chiang, and A. Noureldin, "The utilization of artificial neural networks for multisensor system integration in navigation and positioning instruments," *IEEE Trans. Instrum. Meas.*, vol. 55, no. 5, pp. 1606–1615, 2006.

[17] S. Benkouider, N. Lagraa, M. B. Yagoubi, and A. Lakas, "Reducing complexity of gps/ins integration scheme through neural networks," in *Proc. IEEE IWCMC*, 2013, pp. 53–58.

[18] A. Hiliuta, R. Landry Jr, and F. Gagnon, "Fuzzy corrections in a gps/ins hybrid navigation system," *IEEE Trans. Aerosp. Electron. Syst.*, vol. 40, no. 2, pp. 591–600, 2004.

[19] M. Nguyen-H and C. Zhou, "Improving gps/ins integration through neural networks," *arXiv preprint arXiv:1005.5115*, 2010.

[20] B. Schaffer, G. Kalverkamp, and E. Biebl, "A 2.4 ghz high precision local positioning system based on cooperative roundtrip time of flight ranging," in *Proc. VDE GeMIC*, 2014, pp. 1–4.

[21] B. Xu, L. Shen, F. Yan, and J. Zheng, "Doppler-shifted frequency measurement based positioning for roadside-vehicle communication systems," *Wiley Wireless Commun. Mobile Comput.*, vol. 11, no. 7, pp. 866–875, 2011.

[22] A. Mahmoud, A. Noureldin, and H. S. Hassanein, "Vanets positioning in urban environments: A novel cooperative approach," in *Proc. IEEE VTC (Fall)*, 2015, to appear.

[23] N. Alam, A. Kealy, and A. G. Dempster, "An ins-aided tight integration approach for relative positioning enhancement in vanets," *IEEE Trans. Intell. Transp. Syst.*, vol. 14, no. 4, pp. 1992–1996, 2013.

[24] A. H. Rabiain, A. Kealy, N. Alam, A. G. Dempster, C. Toth, D. Brzezinska, V. Gikas, and R. G. Danezis, Chris, "Cooperative positioning using gps, low-cost ins and dedicated short range communications," in *Proc. ION PNT Meeting*, 2013, pp. 769 – 779.

[25] K. Liu and H. B. Lim, "Positioning accuracy improvement via distributed location estimate in cooperative vehicular networks," in *Proc. IEEE ITSC*, 2012, pp. 1549–1554.

[26] A. Amini, R. M. Vaghefi, J. M. de la Garza, and R. M. Buehrer, "Improving gps-based vehicle positioning for intelligent transportation systems," in *Proc. IEEE IV Symp.*, 2014, pp. 1023–1029.

[27] L. Altoaimy, I. Mahgoub, and M. Rathod, "Weighted localization in vehicular ad hoc networks using vehicle-to-vehicle communication," in *Proc. IEEE GIIS*, 2014, pp. 1–5.

[28] L. Altoaimy and I. Mahgoub, "Fuzzy logic based localization for vehicular ad hoc networks," in *Proc. IEEE CIVTS Symp.*, 2014, pp. 121–128.

[29] M. Rohani, D. Gingras, V. Vigneron, and D. Gruyer, "A new decentralized bayesian approach for cooperative vehicle localization based on fusion of gps and inter-vehicle distance measurements," in *Proc. IEEE ICCVE*, 2013, pp. 473–479.

[30] M. Efatmaneshnik, A. Kealy, A. Tabatabaei Balaei, and A. Dempster, "Cooperative positioning of vehicular networks with a map-matching enabled extended kalman filter," in *Proc. IEEE VTC*, 2010.

[31] A. U. Peker, T. Acarman, C. Yaman, and E. Yuksel, "Vehicle localization enhancement with vanets," in *Proc. IEEE IV Symp.*, 2014, pp. 661–666.

[32] A. Kushki, K. N. Plataniotis, and A. N. Venetsanopoulos, "Intelligent dynamic radio tracking in indoor wireless local area networks," *IEEE Trans. Mobile Comput.*, vol. 9, no. 3, pp. 405–419, 2010.

[33] X. Sheng, Y.-H. Hu, and P. Ramanathan, "Distributed particle filter with gmm approximation for multiple targets localization and tracking in wireless sensor network," in *Proc. ACM/IEEE IPSN*, 2005, pp. 181–188.

[34] L. Lei and S. Qu, "A method of cooperative localization for multiple moving vehicles," *J. Inform. Comput. Sci.*, pp. 707–715, 2014.

[35] A. Bhawiyuga, H.-H. Nguyen, and H.-Y. Jeong, "An accurate vehicle positioning algorithm based on vehicle-to-vehicle (v2v) communications," in *Proc. IEEE ICVES*, 2012, pp. 273–278.

[36] S.-T. Choi, W.-S. Hur, and S.-W. Seo, "Cooperative localization based on topology matching," in *Proc. IEEE WiVeC Symp.*, 2014, pp. 1–5.

[37] N. Alam, A. T. Balaei, and A. G. Dempster, "A dsrc doppler-based cooperative positioning enhancement for vehicular networks with gps availability," *IEEE Trans. Veh. Technol.*, vol. 60, no. 9, pp. 4462–4470, 2011.

[38] N. Drawil and O. Basir, "Intervehicle-communication-assisted localization," *IEEE Trans. Intell. Transp. Syst.*, vol. 11, no. 3, pp. 678–691, 2010.

[39] ——, "Toward increasing the localization accuracy of vehicles in vanet," in *Proc. IEEE ICVES*, 2009, pp. 13–18.

[40] E.-K. Lee, S. Yang, S. Y. Oh, and M. Gerla, "Rf-gps: Rfid assisted localization in vanets," in *Proc. IEEE MASS*, 2009, pp. 621–626.

[41] S. Fujii, A. Fujita, T. Umedu, S. Kaneda, H. Yamaguchi, T. Higashino, and M. Takai, "Cooperative vehicle positioning via v2v communications and onboard sensors," in *Proc. IEEE VTC*, 2011, pp. 1–5.

[42] T. Yan, W. Zhang, G. Wang, and Y. Zhang, "Got: Grid-based on-road localization through inter-vehicle collaboration," in *Proc. IEEE MASS*, 2011, pp. 13–18.

[43] N. Alam, A. Kealy, and A. G. Dempster, "Cooperative inertial navigation for gnss-challenged vehicular environments," *IEEE Trans. Intell. Transp. Syst.*, vol. 14, no. 3, pp. 1370–1379, 2013.

[44] F. Ahammed, J. Taheri, A. Y. Zomaya, and M. Ott, "Vloci: using distance measurements to improve the accuracy of location coordinates in gps-equipped vanets," *Springer Mobile Ubiquit. Syst. Comput. Netw. Serv.*, vol. 73, pp. 149–161, 2012.

[45] F. Ahammed, J. Taheri, A. Zomaya, and M. Ott, "Vloci2: improving 2d location coordinates using distance measurements in gps-equipped vanets," in *Proc. ACM MSWiM*, 2011, pp. 317–322.

[46] K. Golestan, S. Seifzadeh, M. Kamel, F. Karray, and F. Sattar, "Vehicle localization in vanets using data fusion and v2v communication," in *Proc.ACM MSWiM*, 2012, pp. 123–130.

[47] R. Parker and S. Valaee, "Vehicular node localization using received-signal-strength indicator," *IEEE Trans. Veh. Technol.*, vol. 56, no. 6, pp. 3371–3380, 2007.

[48] ——, "Cooperative vehicle position estimation," in *Proc. IEEE ICC*, 2007, pp. 5837–5842.

[49] J. Georgy, A. Noureldin, M. J. Korenberg, and M. M. Bayoumi, "Modeling the stochastic drift of a mems-based gyroscope in gyro/odometer/gps integrated navigation," *IEEE Trans. Intell. Transp. Syst.*, vol. 11, no. 4, pp. 856–872, 2010.

[50] U. Iqbal, T. B. Karamat, A. F. Okou, and A. Noureldin, "Experimental results on an integrated gps and multisensor system for land vehicle positioning," *Hindawi Int. J. Navig. Observation*, vol. 2009.

[51] A. G. Quinchia, G. Falco, E. Falletti, F. Dovis, and C. Ferrer, "A comparison between different error modeling of mems applied to gps/ins integrated systems," *MDPI Sensors*, vol. 13, no. 8, pp. 9549–9588, 2013.

[52] M. Behrisch, L. Bieker, J. Erdmann, and D. Krajzewicz, "Sumo–simulation of urban mobility," in *SIMUL*, 2011.

[53] R. Fuller and X. D. Koutsoukos, *Mobile Entity Localization and Tracking in GPS-less Environnments*. Springer, 2009.

[54] K. P. Valavanis, "Applications of intelligent control to engineering systems intelligent systems, control and automation," Springer, 2009.